The Company of Biologists

RESEARCH ARTICLE

miR-9a mediates the role of Lethal giant larvae as an epithelial growth inhibitor in Drosophila

Scott G. Daniel[1,‡], Atlantis D. Russ[1,2,3,‡], Kathryn M. Guthridge[4], Ammad I. Raina[1], Patricia S. Estes[1], Linda M. Parsons[4,5,*], Helena E. Richardson[4,6,7], Joyce A. Schroeder[1,2,3] and Daniela C. Zarnescu[1,2,3,§]

ABSTRACT

Drosophila lethal giant larvae (lgl) encodes a conserved tumor suppressor with established roles in cell polarity, asymmetric division, and proliferation control. Lgl's human orthologs, HUGL1 and HUGL2, are altered in human cancers, however, its mechanistic role as a tumor suppressor remains poorly understood. Based on a previously established connection between Lgl and Fragile X protein (FMRP), a miRNA-associated translational regulator, we hypothesized that Lgl may exert its role as a tumor suppressor by interacting with the miRNA pathway. Consistent with this model, we found that lgl is a dominant modifier of Argonaute1 overexpression in the eye neuroepithelium. Using microarray profiling we identified a core set of ten miRNAs that are altered throughout tumorigenesis in Drosophila lgl mutants. Among these are several miRNAs previously linked to human cancers including miR-9a, which we found to be downregulated in lgl neuroepithelial tissues. To determine whether miR-9a can act as an effector of Lgl in vivo, we overexpressed it in the context of lgl knockdown by RNAi and found it able to reduce the overgrowth phenotype caused by Lgl loss in epithelia. Furthermore, cross-comparisons between miRNA and mRNA profiling in lgl mutant tissues and human breast cancer cells identified thrombospondin (tsp) as a common factor altered in both fly and human breast cancer tumorigenesis models. Our work provides the first evidence of a functional connection between Lgl and the miRNA pathway, demonstrates that miR-9a mediates Lgl's role in restricting epithelial proliferation, and provides novel insights into pathways controlled by Lgl during tumor progression.

KEY WORDS: miRNA, Epithelial growth, Drosophila

INTRODUCTION

lethal giant larvae (lgl) encodes a conserved tumor suppressor with established roles in cell polarity and proliferation control (Cao et al.,

[1]Department of Molecular and Cellular Biology, University of Arizona, Tucson, AZ 85721, USA. [2]Genetics Graduate Interdisciplinary Program, University of Arizona, Tucson, AZ 85721, USA. [3]Arizona Cancer Center, University of Arizona, Tucson, AZ 85721, USA. [4]Cell Cycle and Development Laboratory, Research Division, Peter MacCallum Cancer Center, Melbourne, Victoria 3000, Australia. [5]Department of Genetics, University of Melbourne, Melbourne, Victoria 3010, Australia. [6]Sir Peter MacCallum Department of Oncology, Department of Anatomy & Neuroscience, Department of Biochemistry & Molecular Biology, University of Melbourne, Melbourne, Victoria 3000, Australia. [7]Department of Biochemistry & Genetics, La Trobe Institute of Molecular Science, La Trobe University, Melbourne, Victoria 3086, Australia.
‡These authors contributed equally to this work *Present address: School of Biological Sciences, Monash University, Melbourne, Victoria 3800, Australia.

§Author for correspondence (zarnescu@email.arizona.edu)

D.C.Z., 0000-0002-9607-0139

2015; Elsum et al., 2012; Froldi et al., 2008; Grifoni et al., 2013; Humbert et al., 2008; Walker et al., 2006). Loss of lgl leads to invasive neural and epithelial tumors accompanied by lethality at the third instar larval stage in Drosophila (Beaucher et al., 2007; Calleja et al., 2016; Gateff, 1978; Merz et al., 1990; Woodhouse et al., 1998). Neural stem cells lacking functional lgl self-renew but fail to differentiate, resulting in stem cell tumors (Ohshiro et al., 2000; Peng et al., 2000). In various types of epithelial cells in Drosophila, lgl, along with discs-large (dlg) and scribbled (scrib), is involved in apico-basal polarity by controlling the appropriate localization of basolateral proteins and adherens junctions (Bilder et al., 2000). Although loss of polarity and overproliferation are separable, overall, in the absence of lgl, epithelial cells lose their monolayer structure as well as the ability to terminally differentiate and instead, overproliferate into neoplastic tumors with invasive characteristics (Froldi et al., 2010, 2008; Grzeschik et al., 2007; Humbert et al., 2008). In neural stem cells, Lgl has been shown to interact with and antagonize the atypical protein kinase C (aPKC)/ PAR polarity complex to control apico-basal polarity and cell proliferation (Betschinger et al., 2003). Likewise, in epithelial tissues, Lgl and aPKC also have antagonistic functions in cell polarity and tissue growth (Bilder et al., 2003; Eder et al., 2005; Tanentzapf and Tepass, 2003). Recently, clonal analyses in the developing eye epithelia have demonstrated that Lgl loss downregulates the Salvador/Warts/Hippo tissue growth control pathway, as well as upregulates the Notch pathway, leading to ectopic cell proliferation and reduced apoptosis (Grzeschik et al., 2010b; Parsons et al., 2014; Portela et al., 2015). Moreover, in lgl mutant wing epithelial tissue, the dMyc transcription factor, and the Hippo, EGFR-Ras-ERK, PI3K-AKT, JNK, Jak-STAT and hypoxia signalling pathways are dysregulated (Grifoni et al., 2015). Additionally, another study showed that Hippo pathway targets, and components of the EGFR, Wingless and Decapentaplegic pathway are elevated, and differentiation is compromised in lgl mutant wing epithelial tissue (Khan et al., 2013).

lgl orthologs have been found in many different species including yeast, worms, zebrafish, mice, and humans (Strand et al., 1995). In mice and humans there are two paralogs each, known as mlgl1/ mlgl2 and HUGL1/HUGL2, respectively. The exogenous expression of the human protein, HUGL1, in flies can rescue the lethality caused by an lgl null mutation, which demonstrates functional conservation across species (Grifoni et al., 2004). Knock-out of the mouse ortholog, mlgl1, results in neuroectodermal tumors and neonatal lethality (Klezovitch et al., 2004), whereas knock-out of mlgl2 causes a branching morphogenesis defect during placental development (Sripathy et al., 2011).

In recent years, aberrant localization and/or reduced expression for either HUGL1 or HUGL2 have been reported in several epithelial cancers including cancer of the breast, stomach, colon, ovary, prostate, skin, endometrium, oesophageal, lung and glioma (Grifoni

Biology Open

et al., 2004; Imamura et al., 2013; Kuphal et al., 2006; Lisovsky et al., 2009, 2010; Liu et al., 2015; Matsuzaki et al., 2015; Nam et al., 2014; Schimanski et al., 2005; Song et al., 2013; Spaderna et al., 2008; Tsuruga et al., 2007). In addition, the locus that contains *HUGL1* (at 17p11.2) is deleted in cases of medulloblastoma (Batra et al., 1995), in early stages of breast cancer (Johnson et al., 2012), and in chromosomally unstable colon cancers (Lassmann et al., 2007). These correlations suggest that in humans, Lgl orthologs may also act as tumor suppressors. Indeed, recent experiments with human breast cancer cells further support this notion, reporting transcriptional regulation of HUGL2 by SNAIL1 and revealing that HUGL2 is a driver of the mesenchymal to epithelial transition (EMT) (Kashyap et al., 2012). Recently, we demonstrated a role for both HUGL1 and HUGL2 in maintaining cell polarity and growth control in human mammary epithelium (Russ et al., 2012). We found that while HUGL1 and HUGL2 inhibited EMT, they also promoted anoikis and polarity in 3-dimensional cultures, as well as inhibited growth of breast cancer cells.

Using genetic interaction experiments in *Drosophila* we have previously identified *lgl* as a dominant modifier of Fragile X protein (FMRP) (Zarnescu et al., 2005), an RNA binding protein implicated in the microRNA (miRNA) pathway (Caudy et al., 2002; Ishizuka et al., 2002). FMRP exhibits physical and genetic interactions with Argonaute 1(AGO1), a core component of the miRNA machinery, which regulates the processing of mature miRNAs (Jin et al., 2004). Given the functional connection between Lgl and FMRP, we hypothesized that Lgl's tumor suppressor function, in addition to its effect on signaling pathways, might also involve regulation of miRNA expression. miRNAs are noncoding RNAs that can control gene expression by inhibiting mRNA translation or by degrading transcripts (Carthew and Sontheimer, 2009). Recently, a large body of evidence has emerged linking dysregulation of miRNA expression to the development and progression of tumors, with miRNAs acting as either oncogenes or tumor suppressors (reviewed in Ventura and Jacks, 2009). For example, *let-7* has multiple cancer-relevant mRNA targets, including those involved in proliferation, differentiation, and stem cell maintenance (reviewed in Boyerinas et al., 2010). This miRNA is highly conserved across species (Pasquinelli et al., 2000) and loss of its expression has been documented in many types of cancer, including breast cancer (Dahiya et al., 2008; O'Hara et al., 2009; Sempere et al., 2007; Takamizawa et al., 2004). *let-7* and several other miRNAs are currently being investigated for potential use as cancer therapeutics (Barh et al., 2010; Hwang and Mendell, 2006; Liu et al., 2008; Tavazoie et al., 2008; Volinia et al., 2006).

Here, using *Drosophila* as a model, we found that *lgl* loss-of-function mutations suppress the *AGO1* overexpression phenotype in the eye, consistent with a functional link between Lgl and the miRNA pathway. Next, we used microarray profiling to identify miRNAs that are misexpressed in neural and epithelial tissues including brain and eye-antennal imaginal discs at different stages of tumor growth in *lgl* loss-of-function mutants. *lgl* mutant larvae are normal sized at the onset of the third instar stage, however at the end of this developmental stage and while wild-type larvae enter pupation, *lgl* larvae continue to grow and accumulate large, invasive imaginal disc and brain tumors (Beaucher et al., 2007; Gateff, 1978; Woodhouse et al., 1998). Thus, the fly provides a unique model of *in vivo* tumorigenesis, whereby neural and epithelial tissues undergo transformation within a few days and importantly, recapitulate several features of metastasis (Beaucher et al., 2007; Calleja et al., 2016; Froldi et al., 2010; Grifoni et al., 2015; Woodhouse et al.,

1998, 1994). We performed our profiling experiments at three different time-points: at tumor onset, during tumor growth, and later, during malignant progression. From these expression profiles, we identified several miRNAs that are dysregulated in *lgl* tumors. Notably, several of the miRNAs we found to be misexpressed in *lgl* mutant tissues have also been linked to human cancers, including *let-7* (Boyerinas et al., 2010), *miR-9a* (Hildebrandt et al., 2010; Lehmann et al., 2008; Zhang et al., 2012) and *miR-210* (Tsuchiya et al., 2011). To evaluate the physiological significance of our findings we began by testing whether *miR-9a* can modulate *lgl*'s phenotypes *in vivo*. Consistent with it being downregulated in *lgl* mutant tumors and functionally important for the *lgl* mutant phenotype, we found that *miR-9a* overexpression reduces the overgrowth phenotype caused by *lgl* loss of function in the wing epithelium. Although the precise mechanism of these genetic interactions remains to be established, here we provide the first evidence of a functional connection between Lgl and the miRNA pathway *in vivo*. Our data show that *miR-9a* mediates at least some aspects of Lgl's role in tumor suppression.

When comparing the miRNAs that are dysregulated throughout the tumorigenesis process, we identified a subset of ten miRNAs that are consistently misexpressed. This core set of miRNAs was further compared to mRNA expression changes in *lgl* mutant neuroepithelial tissues, late in tumorigenesis. Using cross-comparisons between miRNA and mRNA profiling data, we further identified a set of 38 mRNAs that are predicted to be *in vivo* targets of the core set of ten miRNAs dysregulated in *lgl* tumors. GO term and Cytoscape analyses of these mRNAs pinpoint to both established and novel pathways being involved in Lgl-mediated tumor progression. To further determine the significance of our findings in the fly model we identified mRNAs that are altered in an *in vitro* model of cancer based on HUGL1 knock-down in human breast epithelia. When compared with the gene expression profiling in the fly model, we found that *thrombospondin* (*tsp*) is a common factor altered between the fly and human models of tumorigenesis used in our studies. This finding underscores the significance of our combined approach and provides new insights into Lgl's role as a tumor suppressor.

RESULTS

lgl interacts genetically with the miRNA pathway

We have previously shown that Lgl and Fragile X protein (FMRP), an RNA binding protein known as a regulator of the miRNA pathway, form a functional protein complex (Jin et al., 2004; Zarnescu et al., 2005). These findings led us to hypothesize that Lgl may also be involved in regulating the miRNA pathway. To test this possibility, we conducted genetic interaction experiments between *ago1*, a core component of the miRNA machinery, and *lgl* in the *Drosophila* neural epithelium. Overexpression of *AGO1* in the developing retina was previously shown to generate a rough eye phenotype accompanied by depigmentation (Fig. 1A) (Jin et al., 2004). Here, using three independent alleles, i.e. *lgl¹*, *lgl⁴* and *lgl^{U334}*, we found that *lgl* loss-of-function mutations can dominantly suppress the eye phenotype caused by *AGO1* overexpression (Fig. 1). These data support our hypothesis and suggest that *lgl* may modulate the output of the miRNA pathway *in vivo*.

Loss of *lgl* leads to misexpression of specific miRNAs in neuroepithelial tissues

Given the genetic interactions between Lgl and components of the miRNA pathway (Fig. 1), we sought to identify miRNAs that are misexpressed in lgl mutant tissues and thus may provide novel
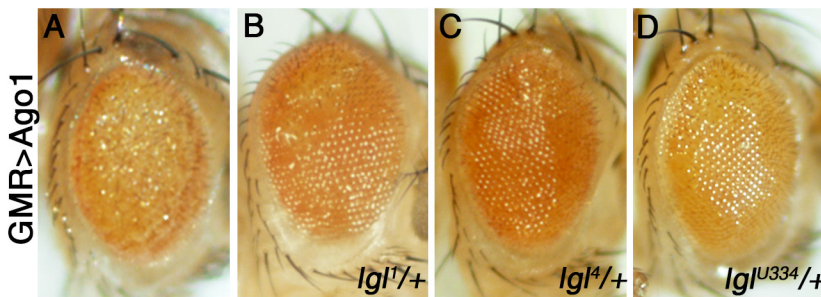
Fig. 1. *lgl* interacts genetically with Argonaute 1 (AGO1) in the eye. (A) Overexpression of *AGO1* using *GMR-Gal4* results in a rough eye phenotype. (B-D) Three independent alleles of *lgl*, namely *lgl¹*, *lgl⁴* and *lgl^U334*, can dominantly suppress the *GMR>AGO1* phenotype. Genotypes as indicated. *N*=at least 10 adults were imaged per genotype.

insights into Lgl's function as a tumor suppressor. To this end, we dissected larval cephalic complexes (i.e. brains and the eye-antennal imaginal discs, which undergo transformation due to loss of lgl) from third instar larvae at three different time points of relevance to the tumor progression process *in vivo*. The first time-point corresponds to the late third instar larval stage (Day 0 in our study), when lgl mutant tissues appear relatively normal, with no signs of overproliferation or loss of polarity compared to wild-type (Fig. 2A,B). For the second time-point, we analyzed lgl mutant larvae three days later (Day 3 in our study) when they appear overgrown and their tissues exhibit visible malformations (Fig. 2C). The third and final time point was chosen after five days (Day 5 in our study) when lgl mutants appear grossly bloated and are filled with tumors that eventually kill the larvae (see Fig. 2D for cephalic complexes at Day 5). Since normal larvae enter pupation after 24 h in the third instar stage, for the second and third time points no wild-type controls were available for comparison, thus the Day 0 wild-type was used as a control throughout. In these studies we compared lgl¹/lgl^U334 mutants to a genomic rescue line as wild-type control (P[lgl⁺];lgl¹/lgl^U334).

To identify miRNAs that are misexpressed in lgl mutant tissues both before and after the onset of aberrant tissue growth, we probed miRNA microarrays with labeled miRNAs isolated from lgl mutants or controls (see Materials and Methods). Three biological replicates (three technical replicates each) were performed. After normalization, differences in the expression of miRNAs were fitted to a linear model that was then used to calculate fold change and statistical significance. Significantly dysregulated miRNAs were determined based on a *P* value cut-off of 0.05, calculated using the Benjamini-Hochberg multiple testing correction (Reiner et al., 2003). Out of 147 miRNAs, we found 38 miRNAs dysregulated in lgl mutants compared to controls at Day 0, 22 at Day 3 and 58 at Day 5 (Table S1). Of these, a core set of 10 miRNAs was found to be consistently dysregulated across all time points: let-7, miR-210, miR-9a, miR-275, miR-1, miR-993, miR-100, miR-1004, miR-980 and miR-317 (Fig. 2E). For validation, the expression levels of let-7, miR-210 and miR-9a in Day 0 lgl mutant tissues were compared to controls using Real-Time PCR with small RNA U6 as a housekeeping gene (data not shown). Expression of all three miRNAs corroborated with the microarray results showing significantly lowered expression in mutant tissues (Table S1). Overall, the majority of altered miRNAs corresponded to mature rather than precursor forms, suggesting that Lgl is not involved in regulation of these targets at a transcriptional level.

Although at this point we do not know whether Lgl regulates the processing of these miRNAs directly or indirectly, via RNA binding proteins such as FMRP or AGO1, our data indicate that loss of *lgl* leads to the dysregulation of specific miRNAs in a temporal manner that corresponds to critical stages of tumor progression including initiation, growth and malignant progression. Furthermore, our findings define an

Lgl-specific 'signature' represented by a core set of ten miRNAs that are dysregulated throughout tumorigenesis and may help elucidate the mechanisms by which Lgl acts as a tumor suppressor.

miR-9a overexpression rescues the overgrowth phenotype of lgl knock-down in the wing epithelium

One of the premises of our work is that the miRNAs found to be dysregulated in *lgl* mutant tissues may mediate Lgl's function as a tumor suppressor. Thus, we hypothesize that restoring the expression of these miRNAs in an *lgl* mutant background might reduce the severity of the mutant phenotype. We began to test this hypothesis by asking whether *miR-9a* or *let-7* overexpression can mitigate *lgl* loss-of-function phenotypes. For these experiments we focused on the wing, where Lgl knock-down by RNAi using the engrailed driver (*en-GAL4*) causes epithelial overgrowth accompanied by an increase in the posterior compartment as compared to the total wing area (with the posterior region defined as wing area posterior to the longitudinal vein L4, see dashed outline in Fig. 3A (Parsons et al., 2017). Additional phenotypes caused by *lgl-RNAi* when driven in the posterior compartment by *en-GAL4* include incomplete cross veins (see insets in Fig. 3B,D and F) and tissue loss, usually near longitudinal vein L4 (data not shown). We could not pursue the *lgl–let-7* interaction due to lethality caused by *let-7* overexpression using *en-GAL4*. Therefore, we focused our studies on the *lgl–miR-9a* functional relationship. Using the *en-GAL4* driver, we overexpressed *miR-9a* in the context of *lgl* knock-down by RNAi and found a statistically significant reduction of the posterior compartment overgrowth caused by *lgl* loss (0.68±0.01 in *en-GAL4; UAS-lgl^RNAi/UAS-miR-9a* compared to 0.732±0.004 in *en-GAL4; UAS-lgl^RNAi*, $P_{value}=2.04×10^{-7}$; see Fig. 3B,D and G). Although overexpression of *miR-9a* alone caused a slight reduction in the wing posterior compartment area compared to *en-GAL4* controls (0.66±0.03 in *en-GAL4; UAS-miR-9a* compared to 0.68± 0.02 in *en-GAL4*; see Fig. 3A,C and G), these findings demonstrate that *miR-9a* overexpression is sufficient to significantly reduce the epithelial overgrowth phenotype caused by *lgl* knock-down in the posterior compartment of the wing. To address potential concerns that the suppression by *miR-9a* may be due to a decrease in GAL4 activity caused by additional *UAS* elements controlling both *miR-9a* and *lgl^RNAi* transgenes, we also compared *en-GAL4 UAS-GFP; UAS-lgl^RNAi* to *en-GAL4; UAS-lgl^RNAi/UAS-miR-9a* and found a similar suppressing effect (0.715±0.003 versus 0.68±0.01, $P_{value}=2.64×10^{-5}$; data not shown). These findings indicate that the overgrowth suppression we detected is not due to a reduction in GAL4 activity but rather due to *miR-9a* expression in the context of *lgl* knock-down. In contrast, *miR-9a* reduction using a loss-of-function allele, *miR-9a^F80*, had no significant effect on posterior compartment size, either on its own (0.68±0.02 in *en-GAL4* compared to 0.69±0.02 in *en-GAL4; miR-9a^F80/+*) or in the context of *lgl^RNAi* (0.722±0.004 in *en-GAL4; UAS-lgl^RNAi/miR-9a^F80*
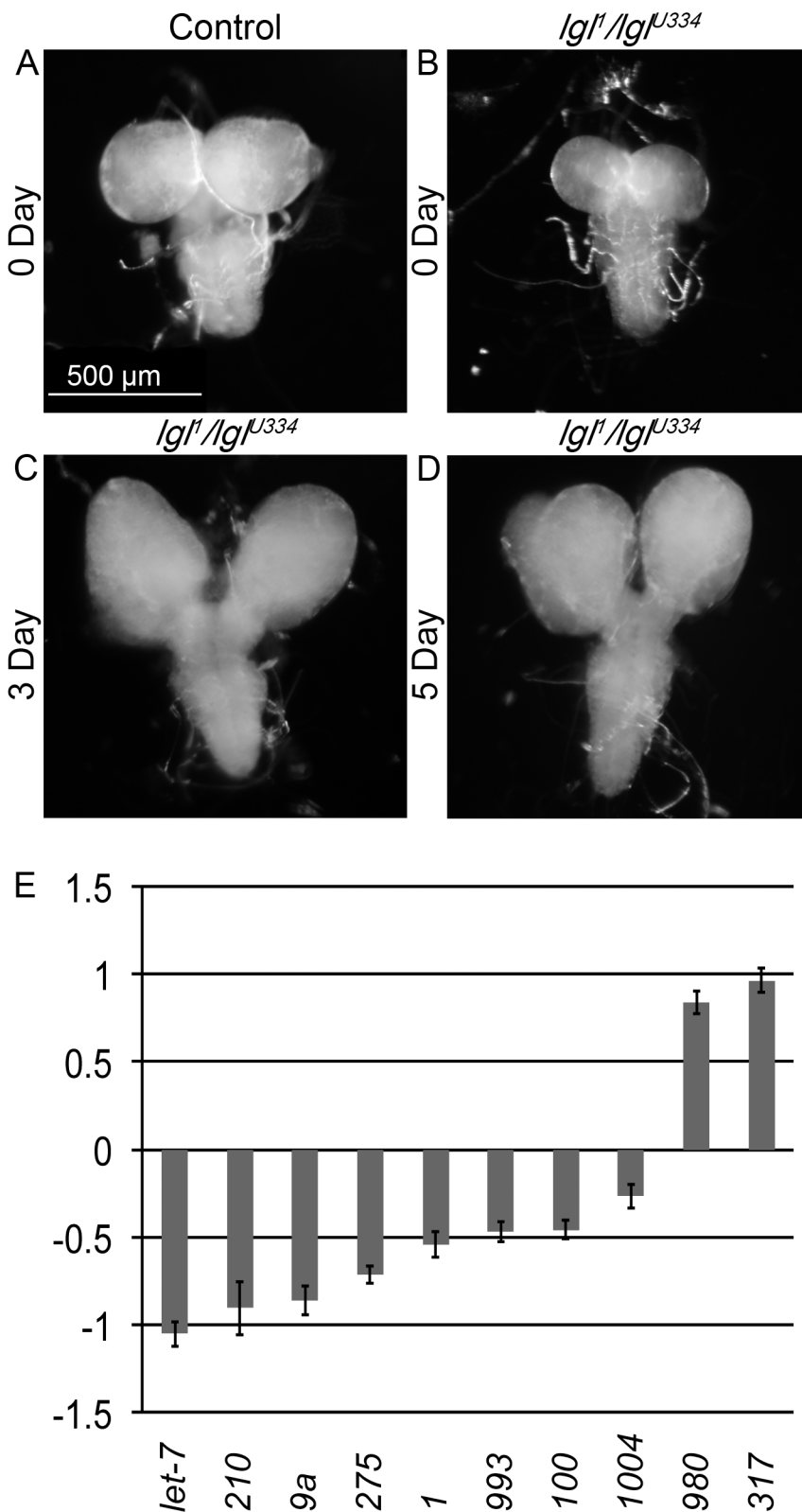
Fig. 2. *lgl* brain tissue and dysregulated microRNAs. (A-D) Cephalic complexes and ventral ganglia of third instar larvae. (A) Day 0 of control's third instar. (B-D) *lgl* mutants do not pupate as normal, day 0, 3, and 5 of *lgl* third instar are shown. (E) Graph of up- and down-regulated microRNAs from microarrays done on tissue from the brains shown in (A-D). Log of fold-change (logFC) is estimated from a linear model of the expression values as computed by the microarray analysis package, limma. The microRNAs listed here, represent ones that were dysregulated across all time-points for mutants, when compared to controls. All microRNAs shown were found to be significantly dysregulated with *P*<0.05, Benjamini-Hochberg multiple testing correction. Error bars show standard error of the mean.

compared to 0.732±0.004 in *en-GAL4; UAS-lgl*^{RNAi} P_{value}=0.09). The failure to observe a genetic interaction in the *miR-9a*^{F80} heterozygous background might indicate that *miR-9a* is abundantly expressed, and reducing its dosage by ∼50% is not sufficient to significantly alter the tissue growth defects due to *lgl* knock-down. To determine whether *miR-9a* overexpression mitigates growth and/or apoptosis defects caused by *lgl* knock-down, we quantified the wing disc size and caspase intensity in third instar wing discs (Fig. S1). These experiments showed a significant increase in caspase activity in the wing pouch, within the en-GAL4 domain for *lgl*^{RNAi} compared to controls (Fig. S1A-G). However, *miR-9a* overexpression did not have a suppressing effect, and the size of
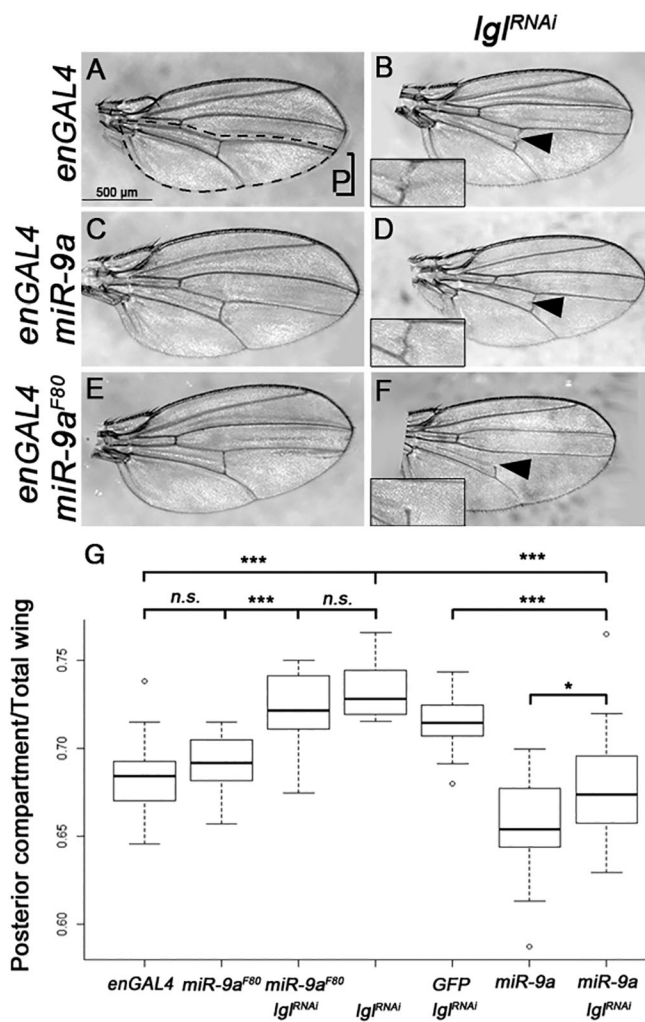
Fig. 3. miR-9a and lgl exhibit genetic interactions in the wing epithelium. (A) en-GAL4 control, posterior compartment P as indicated; (B) en-GAL4; UAS-lgl^{RNAi}; (C) en-GAL4; UAS-miR-9a; (D) en-GAL4; UAS-lgl^{RNAi}/UAS-miR-9a; (E) en-GAL4; miR-9a^{F80}/+; (F) en-GAL4; UAS-lgl^{RNAi}/miR-9a^{F80}. Insets show incomplete cross-vein phenotype. (G) Graph of posterior wing region area divided by total wing area. Genotypes as indicated. ***P<0.001, *P<0.05, n.s., not significant; student's t-test was used to determine statistical significance. For number of wings analysed, see Materials and Methods. Box and whisker plots show median, upper and lower quartiles, highest and lowest points, and outliers.

the posterior compartment was comparable for lgl^{RNAi} miR-9a and lgl^{RNAi} wing discs (Fig. S1A-E,F) suggesting that miR-9a exerts its suppressing effect on lgl^{RNAi} during morphogenesis. Nevertheless, these data provide the first in vivo evidence that restoring miR-9a expression in epithelia can rescue the overgrowth phenotype due to Lgl knock-down. Importantly, these findings are consistent with the miRNA profiling data and support our hypothesis that miRNAs may act as effectors of Lgl's tumor suppressor function in epithelia.

In silico identification of mRNAs targets for the miRNAs dysregulated in lgl mutant tissues

A major challenge in the miRNA field is to identify in vivo target transcripts. Since individual miRNAs can target several mRNAs at once, it is imperative that these transcripts are identified, which should lead to a better mechanistic understanding of the miRNA pathway and the development of therapeutic strategies for diseases

linked to miRNA dysregulation. Several software packages have been developed for predicting mRNA targets of miRNAs, however cell-based assays have shown that about half of the computational predictions do not validate in vivo (Chiang et al., 2010). To address this important issue, we complemented our miRNA microarray data with mRNA profiling experiments. To generate mRNA expression profiles, we compared lgl mutant cephalic tissues dissected from four day old (Day 4) 3rd instar lgl null mutant (lgl^{27S3}/lgl^{E2S31}) (Grzeschik et al., 2007) larvae to wild-type control tissues (w^{1118} larvae at Day 0). After background correction and normalization, any differences in mRNA expression were fitted to a linear model that was then used to calculate fold change and significance of dysregulation. Using a P value cut-off of 0.05 and a logFC cut-off of 1, we identified 169 mRNAs that were significantly dysregulated in mutant tissues versus wild-type (Table S2). For the mRNA microarray data, P values were adjusted using Benjamini-Hochberg multiple testing correction (Reiner et al., 2003). Next, using the miRNA targeting algorithm miRanda (Enright et al., 2003) as implemented by microRNA.org (Betel et al., 2008), we matched the core set of 10 misexpressed miRNAs to the 169 dysregulated mRNA transcripts identified (John et al., 2004).

Given the widely accepted paradigm of mRNA translational repression and mRNA stability by miRNAs (Carthew and Sontheimer, 2009), we matched those miRNAs that were upregulated to predicted mRNA targets that were downregulated (Fig. 4A). Conversely, miRNAs that were found to be downregulated in lgl tissues were matched to upregulated mRNAs. This matching approach allowed us to filter our data and discard: (1) the upregulated mRNAs predicted by microRNA.org to be targeted by upregulated miRNAs, and (2) the downregulated mRNAs predicted to be targeted by downregulated miRNAs. Of the 112 miRNA-mRNA matches predicted (including matches to different sequences within the 3′ UTR for the same gene), 50.9% (57 of 112) were judged to be parsimonious by the filtering method we implemented. Using this approach, we found 38 mRNAs that were both inversely correlated with our core set of ten miRNAs and predicted by microRNA.org to be direct targets (Fig. 4B). For example, miR-980 and miR-317, which were found to be upregulated in lgl tissues, matched 10 downregulated mRNAs. The remaining eight miRNAs, which were downregulated, matched 28 upregulated mRNAs. The strength of the miRNA targeting (mirSVR score, as computed by microRNA.org) as well as the logFC of miRNAs and mRNAs was visualized using Cytoscape (Fig. 5). Notably, our bioinformatics analyses combined with miRNA and mRNA profiling indicate that among the genes identified there are several that have been previously linked to lgl function via standard molecular genetic approaches; Prospero (pros), grainyhead (grh) and castor (cas) are required for proper proliferation and differentiation of neural stem cells, which lgl has also been demonstrated to control (Almeida and Bray, 2005; Bello et al., 2006; Betschinger et al., 2003, 2006; Klezovitch et al., 2004). Interestingly, ft, a transcriptional target of Yki in the Hippo pathway, which is deregulated in lgl mutant tissue (Grifoni et al., 2015; Grzeschik et al., 2010b; Khan et al., 2013), was upregulated in lgl mutant tissue, and is a predicted target for miR-1, suggesting that post-transcriptional regulation of Hippo pathway genes might also be controlled by Lgl.

miRNA and mRNA targets are significantly enriched for GO terms related to hallmarks of cancer

Next, we analyzed the 10 miRNAs and the 38 mRNAs they targeted for gene ontology (GO) terms linked to cancer-related processes using
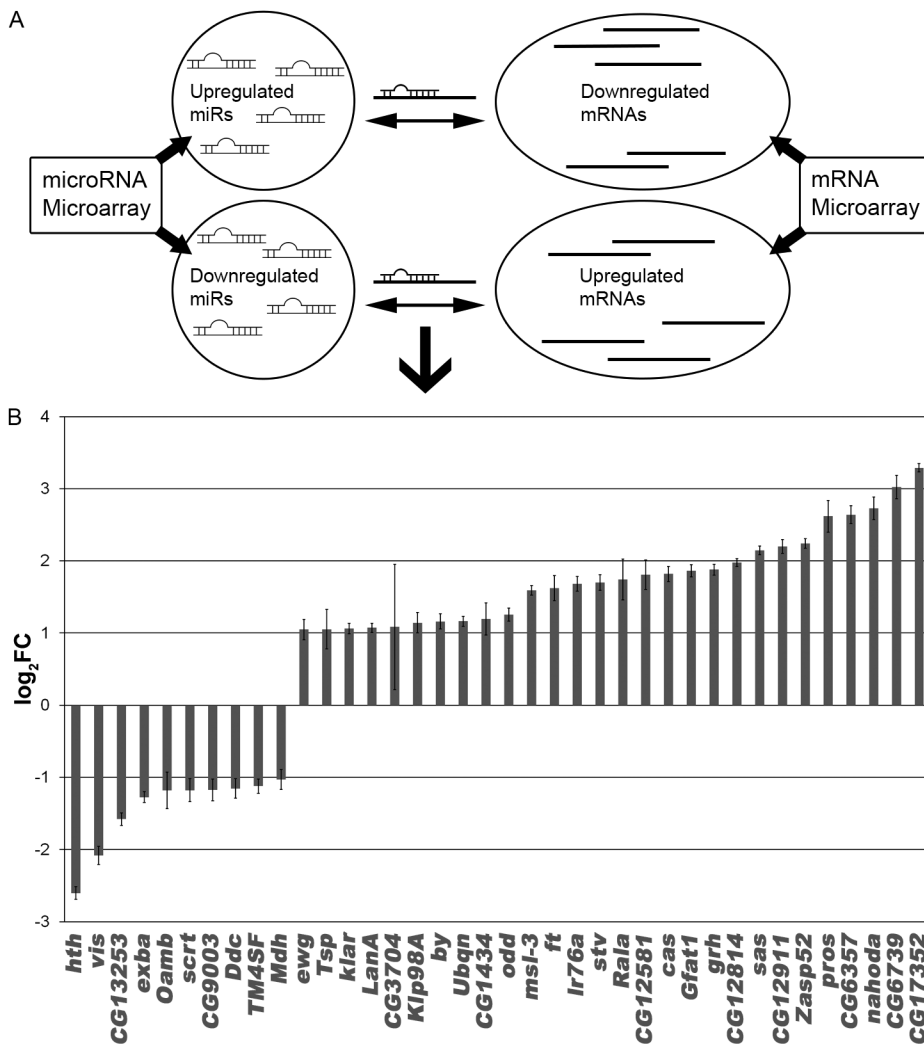
Fig. 4. microRNA targeting strategy and dysregulated mRNAs. (A) Significantly dysregulated microRNAs were matched to mRNAs based on predictions given by the miRanda algorithm. Additionally, matches were validated by their direction of deregulation; upregulated miRNAs matched downregulated mRNAs while downregulated miRNAs matched upregulated mRNAs. (B) The matching mRNAs after applying our targeting strategy (see text). Log of fold-change (logFC) is estimated from a linear model of the expression values as computed by the microarray analysis package, limma. All mRNAs shown were found to be significantly dysregulated with $P<0.05$, Benjamini-Hochberg multiple testing correction. Error bars show standard error of the mean.

the Bingo plug-in for Cytoscape (Maere et al., 2005). Significantly enriched GO terms linked to cancer as determined by processes associated with the disease include cell polarity (e.g. basolateral plasma membrane), cell-cell junctions (e.g. cell-substrate adherens junction, cell-substrate junction), cellular proliferation and differentiation (e.g. ganglion mother cell fate determination, neuron fate commitment, cell fate commitment, etc.) (Hanahan and Weinberg, 2011) (see Table 1). Most notable are cell fate commitment and neuron differentiation, each with eight genes associated. Additional GO terms that were significantly associated with our set of genes include various aspects of development (Table S3). Interestingly, this matching analysis further confirmed cellular processes that have been previously linked to *lgl* loss, such as ganglion mother cell fate determination, cell fate commitment, and basolateral polarity control (Bilder et al., 2000; Khan et al., 2013; Musch et al., 2002; Ohshiro et al., 2000; Peng et al., 2000; Russ et al., 2012).

To predict human cancer pathways potentially affected by absence of HUGL1, we searched Flybase, Genecards miRBase and Ensembl online databases (www.flybase.org, www.genecards.org, www.ensembl.org) for human orthologs of *Drosophila* miRNAs and targets predicted to be altered due to loss of *lgl* (Crosby et al., 2007; Flicek et al., 2008; Safran et al., 2010). Interestingly, of the 14 genes we analyzed, five have human

orthologs with a documented involvement in processes directly or closely linked to cancer (see Table 2; note several similar changes in mRNA expression between brains and wings). Additionally, five of the core set of ten miRNAs matched orthologous human sequences involved in carcinogenesis (see Table 3).

Loss of HUGL1 in human epithelial cells results in upregulation of transcripts linked to breast cancer

To probe the significance of our mRNA and miRNA profiling results for human cancers, we next performed knock-down of HUGL1 in the human mammary epithelial cell line, MCF10A. To silence HUGL1 expression, shRNA sequences designed against *HUGL1* mRNA were optimized in MCF10A cells. Two shRNAs resulted in optimal HUGL1 knock-down and were used in our experiments (Fig. S2). As we have recently shown, loss of HUGL1 alone in MCF10 cells is sufficient to induce overproliferation and loss of apico-basal cell polarity (Russ et al., 2012). The mRNA expression profiles of HUGL1 knock-down cells and shRNA control cells were assessed using a Real Time PCR array (SA Biosciences) containing 84 genes involved in breast cancer. These experiments identified five mRNAs that were significantly upregulated in the HUGL1 knock-down cells as compared to the controls (*ABCG2*, *ESR1*, *KRT19*, *MMP2*, *THBS1*, see Table 4).
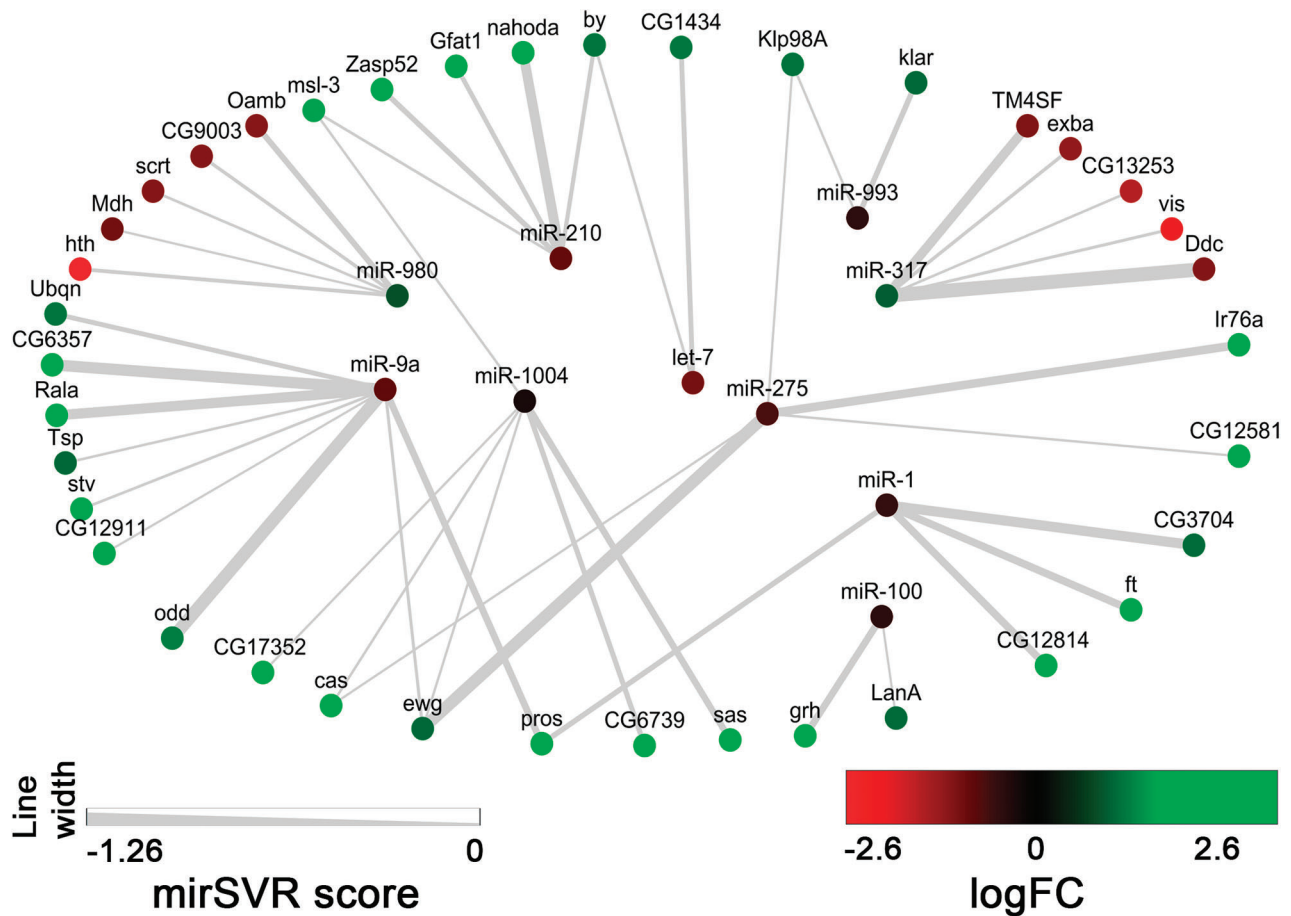
Fig. 5. microRNA targeting network. MicroRNAs (center) target multiple mRNAs (outer ring); in turn, some mRNAs are targeted by a number of microRNAs (e.g. *Klp98A* is targeted by *miR-993* and *miR-275*). The spectrum of maximum downregulation (−2.6 logFC) to maximum upregulation (3.3 logFC) is denoted by a standard red to green gradient. Only upregulated mRNAs are targeted by downregulated microRNAs, while downregulated mRNAs are targeted by upregulated microRNAs. Width of lines connecting microRNA to mRNA represents strength of targeting, as defined by the mirSVR score of the miRanda targeting algorithm. mirSVR score heat map as shown. Green is upregulated, and red is downregulated miRs or genes.

Notably, one of these genes is *THBS1* (*thrombospondin*), which was also identified as an upregulated mRNA in the *Drosophila lgl* mutant tissues and is predicted to be a target of *miR-9a* (see *tsp1* in Fig. 5). These findings underscore the importance of our combined bioinformatics and genetic approach to identify critical genes involved in tumorigenesis driven by Lgl. Future experiments will

focus on the significance of THBS1 in human tumors characterized by HUGL1 loss.

DISCUSSION

Following our previous findings that Lgl regulates the RNA binding protein FMRP (Zarnescu et al., 2005), here we report a novel

Table 1. Genes significantly associated with GO-terms linked to cellular processes dysregulated in cancer including cell polarity, cell fate commitment, differentiation and adhesion

GO-ID	corr *P*-value	Description	Genes in test set
45165	2.17E-02	Cell fate commitment	*stv|hth|cas|Mdh| Rala|exba|pros| grh*
48663	3.05E-03	Neuron fate commitment	*hth|Rala|exba| pros|grh*
7402	2.08E-03	Ganglion mother cell fate determination	*cas|pros|grh*
30182	4.66E-02	Neuron differentiation	*scrt|hth|LanA|Rala|klar|exba|pros|grh*
42706	1.50E-02	Eye photoreceptor cell fate commitment	*hth|Rala|pros| grh*
46552	1.50E-02	Photoreceptor cell fate commitment	*hth|Rala|pros| grh*
1751	1.72E-02	Compound eye photoreceptor cell differentiation	*hth|Rala|klar| pros|grh*
1754	1.82E-02	Eye photoreceptor cell differentiation	*hth|Rala|klar| pros|grh*
46530	2.45E-02	Photoreceptor cell differentiation	*hth|Rala|klar| pros|grh*
5924	1.50E-02	Cell-substrate adherens junction	*Zasp52|by|Tsp*
30055	1.50E-02	Cell-substrate junction	*Zasp52|by|Tsp*
16323	3.64E-02	Basolateral plasma membrane	*Zasp52|by|Tsp*

Corr *P*-value is the significance by Fisher's exact test after Benjamini-Hochberg multiple testing correction. GO-ID's and description are directly drawn from the official GO database (www.geneontology.org) (Ashburner et al., 2000). Genes in test set are those found to be significantly associated (*P* <0.05) with GO-terms. The test set are the ten microRNAs and 38 mRNAs as shown in Fig. 5.

Table 2. Human orthologs and cancer phenotypes linked to mRNAs dysregulated in lgl mutant brain and wing tissues

Gene ID	Full gene name	Direction of regulation	Description of ontology	Human orthologue
Ubqn	Ubiquilin	Up (B)	Heat shock chaperone-binding	UBQLN3 UBQLN1 UBQLN4 UBQLN2
CG6357		Up (B, W)	Cysteine type endopeptidase	
Rala	Ras related protein	Up (B, W)	Ral GTPase, supports tumor initiation and progression, inhibits apoptosis through upregulation of p38 and inhibition of JNK (Sablina et al., 2007). RALB activation restricts initiation of apoptotic programs (Chien et al., 2006).	RALA RALB
Tsp	thrombospondin	Up (B)	Secreted glycoprotein, Integrin-mediated adhesion, may interact with laminin. THBS1 can have tumor suppression or oncogenic effects in cancer in knockout mice (Lopez-Dee et al., 2015; Rodriguez-Manzaneque et al., 2001; Streit et al., 1999).	THBS1,2,3,4 COMP (THBS5)
Stv (CG32130)	starvin	Up (B, W)	Expressed by tendon cells, stress response	
CG12911		Up (B, W)	Function unknown	
odd	odd skipped	Up (B, W)	Zinc finger transcription factor - morphogenesis	OSR2 OSR1
CG17352	Culd, CUB and LDLa domain	Up (B, W)	Low density lipoprotein receptor	
cas	castor	Up (B, W)	Transcription factor for neural cell fate. SRG/CASZ1 is a cell survival gene that controls apoptosis and tumor formation (Yuan et al., 2005).	SRG/CASZ1
ewg	erect wing	Up (B*, W*)	Nuclear respiratory factor 1 – transcription factor positive regulator of Wnt signaling	NRF1
pros	prospero	Up (B, W)	Cell fate determination Human homeobox gene (Zinovieva et al., 1996).	PROX1 PROX2
CG6739		Up (B, W)	Low density lipoprotein receptor	
sas	stranded at second	Up (B)	Fibronectin III domain – axon guidance, morphogenesis	
grh	grainyhead	Up (B)	Ectodermal transcription factor that regulates mitotic activity of neuroblasts. Grainyhead-like 2 enhances the human telomerase reverse transcriptase gene expression by inhibiting DNA methylation at the 5-prime-CpG island in normal human keratinocytes resulting in keratinocyte proliferation and increased cellular life span (Chen et al., 2010).	GRHL1 GRHL2 GRHL3
LanA	laminin A	Up (B)	ECM component, axon guidance	LAMA3
CG12814		Up (B, W)	Function unknown	
ft	fat	Up (B)	Atypical cadherin, Hippo pathway regulator, planar cell polarity	FAT4 DCHS1 DCHS2
CG3704		Up (B)	GPN-loop GTPase XPA binding protein 1	GPN1
CG12581		Up (B)	Function unknown	
Ir76a	Ionotropic receptor 76a	Up (B)	Olfatory receptor – sensory signaling	
klar	klarsicht	Up (B)	Regulation of motor proteins	
Klp98A	Kinesin-like protein at 98A	Up (B, W)	Kinesin KIF1B - susceptibility to neuroblastoma-1 (NBLST1) and to pheochromocytoma	KIF1A KIF1B KIF1C KIF16B
CG1434		Up (B)	Dihydrouridine synthase, Positive regulator of protein synthesis	DUS2L
by	blistery	Up (B, W)	Tensin, localizes at focal adhesions	
nahoda		Up (B, W)	Function unknown	
Gfat1	Glutamine:fructose-6-phosphate aminotransferase 1	Up (B)	Metabolic process	GFPT1 GFPT2
Zasp52 (CG30084)	Z band alternatively spliced PDZ motif protein 52	Up (B)	Muscle structure development	
msl-3	male-specific lethal 3	Up (B)	mRNA binding, Histone H4 acetylation, dosage compensation	MSL3
Ddc	Dopa decarboxylase	Down (B)	Synthesis of bioamines	HDH DDC
vis	vismay	Down (B, W)	Homeobox transcription factor, Transforming growth factor b induced factor 2	TGIF2
CG13253	crimpy	Down (B)	Insulin-like growth factor binding protein (Abu-Safieh et al., 2011).	IGFBPL1 SPINK2,6,1,4,9,7 KAZALD1 IGFBP7 ESM1
		Down (B)	Eukaryotic translation initiation factor	BZW2

Table 2. Continued

Gene ID	Full gene name	Direction of regulation	Description of ontology	Human orthologue
Exba (kra, CG2922)	*extra-bases, krasavietz, eIF-2β*			
TM4SF	*transmembrane 4 superfamily*	Down (B), Up (W)	Tetraspanin EC2 domain Function unknown	
Oamb	*Octopamine receptor in mushroom bodies*	Down (B)	G-protein coupled receptor, ovulation, behavioural	
CG9003		Down (B)	SCF-ubiquitin ligase complex Protein degradation Tissue growth (Yao et al., 2007).	FBXL2 FBXL20 (SCRAPPER)
scrt	*scratch*	Down (B)	Transcriptional repressor of alternative cell fates. Member of Snail family, key regulators of EMT.	SNAI3 SCRT1 SNAI1 SCRT2 SNAI3
Men-b (Mdh)	*malic enzyme b (Malate dehydrogenase)*	Down (B)	Key enzyme in the biosynthesis of lipids	ME3 ME2 ME1
hth	*homothorax*	Down (B, W)	MEIS1 regulates the differentiation, cycling activity, and self-renewal of MLL leukemia cells and functions as a determinant of leukemia stem cell potential (Wong et al., 2007). MEIS1 oncogene is highly expressed in neuroblastoma (Spieker et al., 2001).	MEIS1 MEIS2

B, brain; W; Wing. * indicates that different splice variants of the gene were dysregulated. Comparison between wing and brain gene expression was based on Richardson and Ellul (2014) (https://www.ncbi.nlm.nih.gov/geo/query/acc.cgi?acc=GSE48852). Microarray expression profiles from *Drosophila melanogaster* *scrib* and *lgl* mutant wing imaginal disc and brain complexes at day 9 after egg deposition (AED) versus wild type at day 5 AED.

functional connection between the tumor suppressor Lgl and the miRNA pathway. Although miRNA dysregulation has been linked to cancer progression, the role of this pathway in tumorigenesis remains poorly understood (Iorio and Croce, 2012). As the human orthologs of Lgl, HUGL1 and/or HUGL2, are reported to be downregulated in breast and other epithelial cancers, we turned to the genetically tractable model *Drosophila* to explore the effects of *lgl* loss on the miRNA transcriptome and to identify miRNAs that may act as effectors of *lgl*'s ability to protect against cancer progression by modulating pathways involved in tumorigenesis including cell polarity, proliferation, differentiation, adhesion, cell fate and stem cell expansion.

First, by demonstrating a genetic interaction between *lgl* and *AGO1*, we identified a potential role for Lgl in the microRNA pathway. Next, to identify specific miRNAs misexpressed upon loss of *lgl*, we conducted miRNA microarrays to compare the expression levels of 147 miRNAs in *lgl* mutants compared to wild-type rescue larvae. Through this approach, we identified several miRNAs affected by *lgl* loss during tumor progression (38 for day 0, 32 for day 3, and 75 for day 5). Interestingly, only ten miRNAs were

Table 3. Human orthologs and cancer phenotypes linked to miRNAs dysregulated in lgl mutant tissues

miRNA	Direction of regulation	Homology to human miRNA	Published cancer involvement	Targets in human cancers
miR-210	Down	dme-miR-210 UUGUGCGUGUGACAGCGGCUA hsa-miR-210 CUGUGCGUGUGACAGCGGCUGA	Downregulated in esophageal squamous cell carcinoma and during EMT. It inhibits cancer cell survival and proliferation by inducing cell death and controlling cell cycle arrest. Correlated with differentiated epithelial cells. It may exert tumor suppressive effects through targeting degradation of FGFRL1 (Tsuchiya et al., 2011).	FGFRL1
miR-1	Down	hsa-miR1 UGGAAUGUAAAGAAGUAUGUAU dme-miR1 UGGAAUGUAAAGAAGUAUGGAG	Downregulated in colon cancer. Targets Met expression and modulates Met levels (Migliore et al., 2012).	MET, LASP1, IGF-1, IGFR-1, BCL-2
let-7	Down	hsa-let-7a UGAGGUAGUAGGUUGUAUAGUU dme-let-7 UGAGGUAGUAGGUUGUAUAGU	Defects in let-7 result in lack of terminal differentiation and overproliferation. Loss of let-7 linked to breast cancer via regulation of RAS, Myc, LIN28 or HMGA2 (Bussing et al., 2008).	RAS, MYC, LIN28, HMGA2
miR-100	Down	hsa-miR-100 AACCCGUAGAUCCGAACUUGUG dme-miR-100 AACCCGUAAAUCCGAACUUGUG	miR-100 downregulated in cervical and nasopharyngeal cancer and targets Polo-like kinase 1 (PLK1) (Li et al., 2011; Shi et al., 2010). An upregulation of Plk1 can lead to mitotic catastrophe. Downregulated in oral squamous cell carcinoma (OSCC) and confers loss of sensitivity to ionizing radiation when lost (Henson et al., 2009).	PLK1
miR-9	Down	dme-miR-9a UCUUUGGUUAUCUAGCUGUAUGA hsa-miR-9 UCUUUGGUUAUCUAGCUGUAUGA	Hypermethylated in clear cell renal cell carcinoma, downregulated in gastric carcinoma, (Hildebrandt et al., 2010; Luo et al., 2009; Tränkenschuh et al., 2010)	CDH1, RAB 34 (A Ras family member)

Table 4. Downregulation of HUGL1 in human mammary epithelial cells leads to upregulation of five mRNAs

mRNA	Fold Change	P-value	Function	Drosophila ortholog
ABCG2	2.86	0.019	ATP-Binding Cassette, Sub-Family G (WHITE), Member 2	white
ESR1	5.20	0.021	Estrogen Receptor 1	ERR (Estrogen-related receptor)
KRT19	3.16	0.036	Keratin 19	-
MMP2	5.72	0.025	Matrix Metallopeptidase 2	Mmp2
THBS1	2.70	0.039	Thrombospondin	Tsp (thrombospondin)

Table shows mRNAs upregulated by more than fivefold in HUGL1 knock-down human mammary epithelial cells compared to controls (scrambled knock-down). P values as shown.

consistently affected across all time points studied. This time series enabled us to determine changes in miRNA expression before and during early- as well as late-tumor development that may serve in the future for biomarker development. This approach also provided a robust means for identifying a core set of ten miRNAs that define an Lgl tumor 'signature'. Of the ten *Drosophila* miRNAs identified, *let-7*, *miR-210*, *miR-1*, *miR-100*, and *miR-9a* have homologues in humans as evidenced in miRBase (Griffiths-Jones et al., 2006). These same five have already been shown to exhibit tumor suppressive properties in human cancers (Henson et al., 2009; Iorio and Croce, 2012; Rothé et al., 2011; Volinia et al., 2006; Yu et al., 2007). Among these, *let-7* and *miR-100* are processed from the same primary miRNA.

miR-9a, a known growth regulator (Epstein et al., 2017; Suh et al., 2015), was found to be downregulated in the *lgl* mutant larval epithelial and neural tissues, therefore, we hypothesized that overexpressing *miR-9a* in *lgl* loss-of-function tissues may have a rescuing effect. By restoring levels of *miR-9a* in the wing, flies showed a statistically significant reduction in the overgrowth of the posterior compartment of the wing due to *lgl* knock-down.

We conducted two separate array experiments, one for miRNA and one for mRNA using two different *lgl* mutants. Furthermore, we compared our data to matches predicted by microRNA.org, which uses a machine-learning algorithm to score matches based on sequence similarity, free energy of the RNA duplex, and conservation of the target site. Target-matching algorithms have an estimated 50% error rate and indeed, using one of the latest target matching algorithms implemented by microRNA.org, miRanda, we discovered that the error rate was corroborated by our *in vivo* data. Thus, the power of our combined approach is that of target matches predicted by microRNA.org corresponding with an inverse expression relationship of miRNAs and their predicted mRNA targets in *lgl* mutant tissues (e.g. an upregulated miRNA validates a predicted mRNA target if that mRNA is downregulated). From this analysis, we could link dysregulated miRNAs with mRNAs in *lgl* mutant tissue; in particular, since we have shown that *miR-9a* deregulation contributes to the *lgl* mutant phenotype, these comparisons identify potential protein targets that are important in tumorigenesis upon Lgl depletion.

Cancer is a complex disease affecting many biological processes including: cell growth and proliferation, cell differentiation, angiogenesis, apoptosis, and genomic stability (Hanahan and Weinberg, 2011; Scheel and Weinberg, 2012). The dysregulated miRNAs and mRNAs in our analysis not only corroborated 3′ UTR targeting predicted by microRNA.org, but targeted mRNAs were

significantly associated with GO-terms linked to cellular processes involved in cancer, including cell fate commitment, differentiation, and cell adhesion. Indeed, a disruption in differentiation of neuroblasts has been shown to result in brain tumors, a well-established phenotype of *lgl* mutants (Caussinus and Gonzalez, 2005; Gateff, 1978). Also cell adhesion GO-terms are highly relevant to tumorigenesis, since disruption of cell adhesion is associated with EMT and is critical for cells to break away from the epithelium and become invasive. Future studies will address the contribution of these genes, particularly the *miR-9a* targets, to the *lgl* mutant phenotype.

We have shown that knock-down of HUGL1 in human mammary epithelial cells leads to upregulation of five transcripts that have been linked to cancer stem cells, side population (SP) cells, or increased invasion in cancers (*ABCG2*, *MMP2*, *ESR1*, *THBS1* and *KRT19*; see Table 4). Of these, *ABCG2* (also known as breast cancer resistance protein) is an ATP-binding cassette transporter associated with the cancer stem cell phenotype and chemotherapeutic resistance, including therapy-refractory breast cancer (Ding et al., 2010; Doyle et al., 1998; Zhou et al., 2001). Although two miRNAs, *miR-328* and *miR-519c*, that have been previously described to downregulate human *ABCG2* (Pan et al., 2009; To et al., 2009) have no fly orthologs, we report a reduction in *miR-100*, which is also predicted to bind to the human *ABCG2* 3′UTR (To et al., 2008). Notably, the mature miRNA sequences of *miR-100* have a one base pair difference between human and *Drosophila* as reported by miRBase (Griffiths-Jones et al., 2006). Of the other four mRNAs significantly upregulated in mammary epithelial cells upon HUGL1 knock-down, *MMP2*, a matrix metalloprotease (MMP), is elevated in EMT (Laffin et al., 2008). Upregulation of MMPs has been previously observed in *Drosophila lgl* mutants, conferring invasive abilities, and has also been documented in cancer stem cells (Beaucher et al., 2007; Cronwright et al., 2005; Grifoni et al., 2015; Huang et al., 2011; Na et al., 2011; Woodhouse et al., 1994). In addition, *ESR1* is associated with aggressive breast tumor types, and *KRT 19* has been implicated as a marker of circulating tumor cells (Kim et al., 2011). Interestingly, *THBS1*, thrombospondin which regulates remodeling of the extracellular matrix (Huang et al., 2017), is an orthologue of *tsp*, a fly mRNA that we report upregulated in *lgl* mutants. This upregulation is potentially due to the reduction in *miR-9a* levels we detected, as *tsp* is a predicted target of this miRNA (Sampson et al., 2007; Selbach et al., 2008).

let-7, the most significantly downregulated miRNA in *lgl* tissues, has been shown to inhibit breast cancer cell proliferation in severely compromised immunodeficient (SCID) mice while its loss led to increased stem cell renewal (Yu et al., 2007). It was also shown to act as a repressor of stemness and is frequently lost in transformation (reviewed in Büssing et al., 2008). Similarly, in *Drosophila*, *let-7* is associated with cell differentiation and is regulated by the steroid hormone receptor, EcR (Caygill and Johnston, 2008; Kucherenko et al., 2012; Wu et al., 2012), and therefore its down-regulation would be expected to result in the accumulation of cells in a progenitor-like state. *miR-9* is downregulated in human gastric carcinoma, breast cancer, and ovarian cancer, and has been shown to exhibit control over cell proliferation and metastasis (Laios et al., 2008; Lujambio et al., 2008; Luo et al., 2009; Selcuklu et al., 2012). The findings presented here, coupled with an established role for Lgl as a regulator of stem and epithelial cell integrity in *Drosophila*, suggest that similar miRNAs and downstream pathways may be dysregulated in both fly and human tumors with loss of Lgl or HUGL1/2, respectively. We speculate that the contribution of *lgl* as

a tumor suppressor may be attributed to its control over epithelial cell plasticity and localization of cell fate determinants, and/or by conferring protection against a dedifferentiated cancer stem cell population. Proper regulation of miRNAs *let-7* and *miR-9* by *lgl* via modulation of miRNA processing could contribute to this role.

In summary, we used a combined approach including bioinformatics in flies and human cells lacking Lgl and identified a 'signature' set of miRNAs characteristic to Lgl tumors. Cross comparisons between miRNA and mRNA profiling uncovered a small set of mRNAs that are both dysregulated *in vivo* and represent putative targets of the signature miRNAs. Although Lgl has been implicated in regulating endocytosis (Parsons et al., 2014; Portela et al., 2015) and non-muscle Myosin (Strand et al., 1994), our study suggests that Lgl might also regulate through its binding to FMRP (Zarnescu et al., 2005) the level of specific microRNAs, which would then affect the expression of various mRNAs including those involved in signaling pathways known to be deregulated by *lgl* impairment (Grifoni et al., 2015; Grzeschik et al., 2010a; Khan et al., 2013; Parsons et al., 2014). Among the dysregulated mRNAs, thrombospondin, a component of the extracellular matrix, was found to be misexpressed in both flies and human cells lacking Lgl. It is tempting to speculate that this connection between Lgl depletion and thrombospondin upregulation points to a mechanism involving the remodeling of the extracellular matrix, a key player in metastasis, which will be explored in future experiments. These results, together with genetic interaction experiments in *Drosophila*, suggest the potential for using miRNAs as therapeutics in tumors with Lgl loss.

MATERIALS AND METHODS
Drosophila genetics
All flies were raised on standard fly food at 25°C, except where otherwise noted. *lgl* alleles were previously described (Grzeschik et al., 2007; Zarnescu et al., 2005). *lgl* stocks were balanced over *Kr:GFP-CyO*. *UAS-lgl^{RNAi}* stocks were obtained from the Vienna *Drosophila* RNAi Center (lines # v51247 and v51249). *UAS miR-9a* and *miR-9a^{F80}* flies were provided by Fen-Biao Gao (University of Massachusetts Medical School, MA, USA) and Eric Lai (Sloan-Kettering Cancer Center, NY, USA). *UAS-let-7* was obtained from Laura Johnston (Columbia University, NY, USA). *en-GAL4, GMR-GAL4*, and *UAS-GFP* were obtained from the Bloomington Stock Center (http://flystocks.bio.indiana.edu/). A recombinant stock containing *UAS-lgl-RNAi^{51247}* and *UAS-lgl-RNAi^{51249}* (third chromosome) was generated and a stock made with *en-GAL4* (second chromosome).

Adult wing and eye sample preparations
A recombinant stock containing *UAS-lgl-RNAi^{51247}* and *UAS-lgl-RNAi^{51249}* (third chromosome) was generated and a stock made with *en-GAL4* (second chromosome). Wings of *en-GAL4/+; UAS-lgl^{RNAi}/+, en-GAL4/+; UAS-lgl^{RNAi}/UAS-miR-9a, en-GAL4/+; UAS-lgl^{RNAi}/miR-9a^{F80}* were removed under a dissecting light microscope and mounted on standard glass slides. Slides were scored for defects and examples of phenotypes were imaged using an Olympus DP71 imaging camera on a Leica MZ6 microscope. For *en-GAL4/+; UAS-lgl^{RNAi}/+*, we scored *n*=132 wings. For *en-GAL4/+; UAS-lgl^{RNAi}/UAS-miR-9a*, *n*=186. For *en-GAL4/+; UAS-lgl^{RNAi}/miR-9a^{F80}*, *n*=98 wings. For *en-GAL4/+; +/+*, *n*=140 wings. For *en-GAL4/+; UAS-miR-9a/+*, *n*=77 wings. For *en-GAL4/+; miR-9a^{F80}*, *n*=70 wings. For *en-GAL4, UAS-GFP; UAS-lgl^{RNAi}/+*, *n*=32. For *en-GAL4, UAS-GFP/+,+*, *n*=50. Images were processed using Adobe Photoshop and the posterior wing region as a proportion of total wing area was measured using ImageJ. The posterior wing region was defined as wing area posterior to the longitudinal vein L4. 'Freehand selection' was used to capture pixel areas and 'Measure' was used to compute the areas. For quantifying posterior wing region ratios we used a subset of samples: for *en-GAL4/+; UAS-lgl^{RNAi}/+*, we imaged and measured *n*=16 wings. For *en-GAL4/+; UAS-lgl^{RNAi}/UAS-miR-9a*, *n*=20. For *en-GAL4/+; UAS-lgl^{RNAi}/miR-9a^{F80}*, *n*=20

wings. For *en-GAL4, UAS-GFP/+; UAS-lgl^{RNAi}/+* we imaged *n*=28 wings. For statistics, measurements within genotypes were checked for normality using the ad.test() in R. Differences between genotypes were calculated using t.test() in R for parametric distributions and wilcox.test() for non-parametric distributions. All tests used default options.

For adult eyes, flies were collected and imaged in the first 1-2 days after eclosion. Images were acquired using an Olympus DP71 camera mounted on a Leica MZ6 microscope and processed with ImageJ and Adobe Photoshop. For all genotypes we imaged 10-20 randomly selected flies (males and females).

Brain dissection and imaging
Homozygous larvae were selected against GFP expression under UV light with a Leica MZ8 microscope and washed 3 times in 1× PBS. Cephalic complexes, consisting of brain lobes, ventral ganglion, and eye imaginal discs, were dissected from larvae and suspended in a drop of 1× PBS for imaging. Brain images were obtained using an Olympus DP71 imaging camera mounted on a Leica MZ6 microscope and processed with Adobe Photoshop.

RNA preparation, microarrays and RT-PCR validation
For miRNA analysis, cephalic complexes were dissected from 20 third instar larvae per genotype and were pooled to create each time point sample. Three samples were collected per time point and total RNA was immediately extracted following dissection with a miRVana RNA extraction kit to conserve small RNA according to manufacturer's protocols (Ambion, Austin, TX, USA). RNA was quantified and evaluated for integrity with a nanodrop spectrophotometer and denaturing agarose gels.

For miR microarray analysis, total RNA was shipped to Genosensor (Phoenix, AZ, USA) where it was subjected to quality testing, hybridized with fluorescent probes and washed over an array spotted with cDNA complementary to 147 published *Drosophila* miRNAs. Fluorescence was imaged with a GenePix 4000B microarray scanner and measured using GenePix Pro 5.0.0.49 software.

To validate microarray results, Real-Time PCR was performed on select miRNAs. 1 µg RNA was annealed to poly (A) linkers and reverse transcribed with a one-step cDNA Synthesis Kit (GenoSensor, Phoenix, AZ, USA) according to manufacturer's protocols. Real-Time SYBR green Master Mix was combined with amplified cDNA and validated Real Time primers for *Drosophila let-7*, *miR-9a*, *miR-210*, and *U6* (GenoSensor, Phoenix, AZ, USA). Real-Time amplification reactions were loaded into a 384-well plate and run on an ABI 7900 Real Time thermocycler with an initial denaturation of 15 min at 94°C, 30-45 cycles of denaturation at 94°C for 30 s, annealing at 59°C for 15 s, and elongation 72°C for 30 s. Raw data was processed using a common threshold value. Fold changes were calculated with the delta delta Ct method using U6 as a housekeeping gene.

For mRNA analysis, RNA was isolated from 20 cephalic complexes (brain lobes and eye discs). Samples were from: wild-type day 0 third instar larvae and day 4 *lgl^{27S3/E2S31}* mutant third instar larvae. 1 µg of total RNA was used for template preparation as per manufacturer's instructions, and hybridized to an Affymetrics 2.0 microarray gene chip. Gene-chips were washed and stained in the Affymetrix Fluidics Station 400 and scanned using the Hewlett-Packard GeneArray Scanner G2500A.

Cell culture
MCF10A cell lines were obtained from American Type Culture Collection (ATCC) and cultured in Dulbecco's modified Eagle medium/F12 (DMEM/F12) supplemented with 5% Horse Serum (Invitrogen), 10 µg/ml insulin, 100 ng/ml Cholera toxin (Sigma Aldrich), 20 ng/ml Epidermal Growth Factor, 1% Penicillin-Streptomycin (Cellgro), and 0.5 µg/ml Hydrocortisone. All cells were grown at 37°C in 5% CO_2. They were recently authenticated (Russ et al., 2012) and checked for contamination.

Viral shRNA transductions
MISSION shRNA lentiviral particles containing nontarget control shRNA or *HUGL1* shRNAs and packaging vectors were purchased from Sigma Aldrich (NM_004140, clones TRCN0000117137-141). For transduction, virus was added to MCF10A cells at a multiplicity of infection (MOI) range of 1 to 3 in the presence of 8 µg/ml hexadimethrine bromide (Sigma

Aldrich) in culture medium. Transduced cells were selected using puromycin dihydrochloride (Sigma Aldrich) at 2 µg/ml. Stable lines were used as heterogenous populations; clones were not selected.

Real time PCR array

Total RNA was isolated from the MCF10A control and *HUGL1* shRNA cell lines two weeks after transduction using the RNeasy kit from Qiagen (Valencia, CA, USA). Total RNA concentration and purity in the eluted samples was tested using a NanoDrop spectrophotometer (NanoDrop Technologies). RNA quality was examined in 1% denaturing agarose gels and sharp bands at 18S and 28S ribosomal were verified. Following RNA preparation, the samples were treated with DNase using the RNase-Free DNase Set (Qiagen) to ensure elimination of genomic DNA, and the extracted RNA was converted to cDNA using the RT^2 First Strand Kit (Qiagen) following manufacturer's instructions. cDNA was stored at −20°C until used for gene expression profiling.

The RT^2 Profiler PCR Array System (SABiosciences, Qiagen) was used to evaluate the cell lines for differential gene expression. The genes evaluated in this Breast Cancer RT PCR array include multiple genes involved in breast cancer carcinogenesis. SYBR based Real-time PCR detection was carried out per the manufacturer's instructions. The array was cycled on an ABI 7900HT real-time cycler on the following program: 1 cycle of 10 min at 95°C followed by 40 cycles of 15 s at 95°C and 1 min at 60°C. Raw data were processed in ABI software using similar baseline and threshold values and exported to a template Excel file (Microsoft) for analysis. Analyses of the raw C_T values were conducted using the $\Delta\Delta C_T$ method through the SABiosciences Data Analysis Web Portal (www.sabiosciences.com). Runs that did not pass quality control tests were eliminated and four replicates of each treatment were used for statistical analysis.

Western blots

Cultured cells were lysed in ice-cold lysis buffer containing 20 mM TRIS pH 7.5, 150 mM NaCl, 1% NP40, 5 mM EDTA pH 8.0, 1% NaF, 1% $NaVO3$, 0.1% NH_4 Molybdate and 8% Complete phosphatase and protease inhibitor (Roche). The lysates were centrifuged at 13,000 rpm for 10 min at 4°C and supernatant was collected for western blot analysis. 20µg protein lysate was separated by SDS-PAGE (7%) and transferred to PVDF membrane (Millipore). The membrane was blocked in 5% milk in PBS/ 0.1% Tween solution and then used for immunoblotting. The primary antibodies, anti-HUG1 (911-1010, cat # H00003996-M01) and anti-β-actin (AC-74) were purchased from Abnova and Sigma, respectively and the secondary antibody, conjugated to horseradish peroxidase (HRP), goat anti-mouse IgG HRP was purchased from Invitrogen/Molecular Probes. Proteins on the membrane were treated with Super Signal Chemiluminescent Substrate (Pierce), visualized on Imagetech-B film (American X-ray) and developed with a Konica SRX-101C.

Microarray analysis, microRNA target matching and GO-term analysis

Both microarrays (microRNA and mRNA) were analysed using the Bioconductor package in the R statistical software environment. For microRNAs, normalization was done between arrays and correlation was determined for technical replicates. Normalization was done for arrays on a comparison group basis (i.e. for the day 3 lgl[1]/lgl[U334] compared to day 0 wild-type only those two groups were normalized rather than all). For mRNAs, background correction and normalization was done using the robust-multichip-array (rma) algorithm (Parrish and Spencer, 2004). Data for both experiments were then fitted to separate linear models using the limma package (Wettenhall and Smyth, 2004), which calculated fold changes and *P*-values (using Benjamini-Hochberg multiple testing correction).

Computationally determined targets with good mirSVR scores and conservation across species were downloaded from microRNA.org. This list was filtered for the miRNAs of interest and the predicted targets were matched to mRNAs of interest. Upregulated miRNAs were matched only to downregulated mRNAs and vice versa. The targeting network was visualized using Cytoscape software version 2.8.3 (Shannon et al., 2003). The Bingo plug-in (version 2.44) for Cytoscape was then used to compute enrichment for GO-terms of the miRNAs and mRNAs together (Maere et al., 2005). The background used for enrichment tests consisted of all miRNAs and predicted targets of the same aforementioned list from microRNA.org. Fisher exact tests were used with Benjamini-Hochberg multiple testing correction to determine if groups of miRNAs/mRNAs were significantly associated with a specific GO-term. Only those with a corrected *P*-value of 0.05 or less were included in the results.

Wing imaginal disc immunostaining and quantification

Wing discs were dissected from wandering third instar larve in Grace's medium (source) and incubated for 1 h to incorporate a BrDU analog, EdU, using the Click-iT Kit (Invitrogen). Discs were fixed in 3.5% formaldehyde in PBS, pH 7.2, permeabilized with 0.1% Triton, blocked with 3% BSA, and labeled. The presence of cleaved caspase was detected using Dcp-1 Antibody (Cell Signaling, #9578) at 1/500 dilution, and detected with anti-rabbit Alexa-647 at 1/750. Anti-GFP-FITC (Rockland, #600-402-215) was used at 1/200 dilution and Hoechst 33344 (Life Technologies) at 1/10,000. Discs were mounted in 4% n-propyl gallate in glycerol and imaged on a Zeiss 510 Meta Confocal Microscope. Images were processed by Adobe Photoshop. Total wing disc and the engrailed domain (GFP positive) were defined with the 'magnetic lasso' tool. For the measurements shown in Fig. S1E, to reduce background noise, only the top-most epithelial layer corresponding to the wing pouch was measured. For statistics, measurements within genotypes were checked for normality using the shapiro.test() in R. Differences between genotypes were calculated using t.test() in R. All tests used default options.

Statistical analyses

Statistical analyses are as described for individual methods.

Author contributions

Conceptualization: D.C.Z., S.G.D., A.D.R., L.M.P., H.E.R., J.A.S.; Methodology: D.C.Z., S.G.D., A.D.R., L.M.P., H.E.R., J.A.S.; Software: S.G.D.; Validation: D.C.Z., S.G.D., A.D.R., L.M.P., J.A.S.; Formal analysis: D.C.Z., S.G.D., A.D.R., K.M.G., L.M.P., H.E.R., J.A.S.; Investigation: S.G.D., A.D.R., A.I.R., P.S.E., L.M.P.; Resources: D.C.Z., H.E.R., J.A.S.; Data curation: S.G.D., K.M.G.; Writing - original draft: D.C.Z., S.G.D., A.D.R.; Writing - review & editing: D.C.Z., H.E.R.; Visualization: D.C.Z., S.G.D., A.D.R.; Supervision: D.C.Z., H.E.R., J.A.S.; Project administration: D.C.Z.; Funding acquisition: D.C.Z., H.E.R., J.A.S.

Data availability

Fly stocks are available upon request.
All microarray and bioinformatics analyses have been deposited in GEO: GPL15976 (*Drosophila* 147 microRNA version 13), GSE40293 (microRNA microarray of *Drosophila melanogaster* extracted from cephalic complexes of *lgl*-hypomorph third instar larvae), GSE40294 [mRNA microarray of *Drosophila melanogaster* extracted from cephalic complexes of lgl27S3/lglE2S31 (*lgl*-null) and FRT82B (wild-type) third instar larvae] and GSE40295 (genetic and bioinformatics approaches to decipher LGL's function as a tumor suppressor).

Supplementary information

Supplementary information available online at
http://bio.biologists.org/lookup/doi/10.1242/bio.027391.supplemental

References

Abu-Safieh, L., Abboud, E. B., Alkuraya, H., Shamseldin, H., Al-Enzi, S., Al-Abdi, L., Hashem, M., Colak, D., Jarallah, A., Ahmad, H. et al. (2011). Mutation of IGFBP7 causes upregulation of BRAF/MEK/ERK pathway and familial retinal arterial macroaneurysms. *Am. J. Hum. Genet.* **89**, 313-319.

Almeida, M. S. and Bray, S. J. (2005). Regulation of post-embryonic neuroblasts by Drosophila Grainyhead. *Mech. Dev.* **122**, 1282-1293.

Ashburner, M., Ball, C. A., Blake, J. A., Botstein, D., Butler, H., Cherry, J. M., Davis, A. P., Dolinski, K., Dwight, S. S., Eppig, J. T. et al. (2000). Gene ontology: tool for the unification of biology. The Gene Ontology Consortium. *Nat. Genet.* **25**, 25-29.

Barh, D., Malhotra, R., Ravi, B. and Sindhurani, P. (2010). MicroRNA let-7: an emerging next-generation cancer therapeutic. *Curr. Oncol.* **17**, 70-80.

Batra, S. K., McLendon, R. E., Koo, J. S., Castelino-Prabhu, S., Fuchs, H. E., Krischer, J. P., Friedman, H. S., Bigner, D. D. and Bigner, S. H. (1995). Prognostic implications of chromosome 17p deletions in human medulloblastomas. *J. Neurooncol.* **24**, 39-45.

Beaucher, M., Goodliffe, J., Hersperger, E., Trunova, S., Frydman, H. and Shearn, A. (2007). Drosophila brain tumor metastases express both neuronal and glial cell type markers. *Dev. Biol.* **301**, 287-297.

Bello, B., Reichert, H. and Hirth, F. (2006). The brain tumor gene negatively regulates neural progenitor cell proliferation in the larval central brain of Drosophila. *Development* **133**, 2639-2648.

Betel, D., Wilson, M., Gabow, A., Marks, D. S. and Sander, C. (2008). The microRNA.org resource: targets and expression. *Nucleic Acids Res.* **36**, D149-D153.

Betschinger, J., Mechtler, K. and Knoblich, J. A. (2003). The Par complex directs asymmetric cell division by phosphorylating the cytoskeletal protein Lgl. *Nature* **422**, 326-330.

Betschinger, J., Mechtler, K. and Knoblich, J. A. (2006). Asymmetric segregation of the tumor suppressor brat regulates self-renewal in Drosophila neural stem cells. *Cell* **124**, 1241-1253.

Bilder, D., Li, M. and Perrimon, N. (2000). Cooperative regulation of cell polarity and growth by Drosophila tumor suppressors. *Science* **289**, 113-116.

Bilder, D., Schober, M. and Perrimon, N. (2003). Integrated activity of PDZ protein complexes regulates epithelial polarity. *Nat. Cell Biol.* **5**, 53-58.

Boyerinas, B., Park, S.-M., Hau, A., Murmann, A. E. and Peter, M. E. (2010). The role of let-7 in cell differentiation and cancer. *Endocr Relat. Cancer* **17**, F19-F36.

Büssing, I., Slack, F. J. and Grosshans, H. (2008). let-7 microRNAs in development, stem cells and cancer. *Trends Mol. Med.* **14**, 400-409.

Calleja, M., Morata, G. and Casanova, J. (2016). Tumorigenic properties of Drosophila epithelial cells mutant for lethal giant larvae. *Dev. Dyn.* **245**, 834-843.

Cao, F., Miao, Y., Xu, K. and Liu, P. (2015). Lethal (2) giant larvae: an indispensable regulator of cell polarity and cancer development. *Int. J. Biol. Sci.* **11**, 380-389.

Carthew, R. W. and Sontheimer, E. J. (2009). Origins and mechanisms of miRNAs and siRNAs. *Cell* **136**, 642-655.

Caudy, A. A., Myers, M., Hannon, G. J. and Hammond, S. M. (2002). Fragile X-related protein and VIG associate with the RNA interference machinery. *Genes Dev.* **16**, 2491-2496.

Caussinus, E. and Gonzalez, C. (2005). Induction of tumor growth by altered stem-cell asymmetric division in Drosophila melanogaster. *Nat. Genet.* **37**, 1125-1129.

Caygill, E. E. and Johnston, L. A. (2008). Temporal regulation of metamorphic processes in Drosophila by the let-7 and miR-125 heterochronic microRNAs. *Curr. Biol.* **18**, 943-950.

Chen, W., Dong, Q., Shin, K.-H., Kim, R. H., Oh, J.-E., Park, N.-H. and Kang, M. K. (2010). Grainyhead-like 2 enhances the human telomerase reverse transcriptase gene expression by inhibiting DNA methylation at the 5′-CpG island in normal human keratinocytes. *J. Biol. Chem.* **285**, 40852-40863.

Chiang, H. R., Schoenfeld, L. W., Ruby, J. G., Auyeung, V. C., Spies, N., Baek, D., Johnston, W. K., Russ, C., Luo, S., Babiarz, J. E. et al. (2010). Mammalian microRNAs: experimental evaluation of novel and previously annotated genes. *Genes Dev.* **24**, 992-1009.

Chien, Y., Kim, S., Bumeister, R., Loo, Y.-M., Kwon, S. W., Johnson, C. L., Balakireva, M. G., Romeo, Y., Kopelovich, L., Gale, M.Jr et al. (2006). RalB GTPase-mediated activation of the IkappaB family kinase TBK1 couples innate immune signaling to tumor cell survival. *Cell* **127**, 157-170.

Cronwright, G., Le Blanc, K., Götherström, C., Darcy, P., Ehnman, M. and Brodin, B. (2005). Cancer/testis antigen expression in human mesenchymal stem cells: down-regulation of SSX impairs cell migration and matrix metalloproteinase 2 expression. *Cancer Res.* **65**, 2207-2215.

Crosby, M. A., Goodman, J. L., Strelets, V. B., Zhang, P. and Gelbart, W. M. (2007). FlyBase: genomes by the dozen. *Nucleic Acids Res.* **35**, D486-D491.

Dahiya, N., Sherman-Baust, C. A., Wang, T.-L., Davidson, B., Shih, I.-M., Zhang, Y., Wood, W., III, Becker, K. G. and Morin, P. J. (2008). MicroRNA expression and identification of putative miRNA targets in ovarian cancer. *PLoS ONE* **3**, e2436.

Ding, X.-W., Wu, J.-H. and Jiang, C.-P. (2010). ABCG2: a potential marker of stem cells and novel target in stem cell and cancer therapy. *Life Sci.* **86**, 631-637.

Doyle, L. A., Yang, W., Abruzzo, L. V., Krogmann, T., Gao, Y., Rishi, A. K. and Ross, D. D. (1998). A multidrug resistance transporter from human MCF-7 breast cancer cells. *Proc. Natl. Acad. Sci. USA* **95**, 15665-15670.

Eder, A. M., Sui, X., Rosen, D. G., Nolden, L. K., Cheng, K. W., Lahad, J. P., Kango-Singh, M., Lu, K. H., Warneke, C. L., Atkinson, E. N. et al. (2005). Atypical PKCiota contributes to poor prognosis through loss of apical-basal polarity and cyclin E overexpression in ovarian cancer. *Proc. Natl. Acad. Sci. USA* **102**, 12519-12524.

Elsum, I., Yates, L., Humbert, P. O. and Richardson, H. E. (2012). The Scribble-Dlg-Lgl polarity module in development and cancer: from flies to man. *Essays Biochem.* **53**, 141-168.

Enright, A. J., John, B., Gaul, U., Tuschl, T., Sander, C. and Marks, D. S. (2003). MicroRNA targets in Drosophila. *Genome Biol.* **5**, R1.

Epstein, Y., Perry, N., Volin, M., Zohar-Fux, M., Braun, R., Porat-Kuperstein, L. and Toledano, H. (2017). miR-9a modulates maintenance and ageing of Drosophila germline stem cells by limiting N-cadherin expression. *Nat. Commun.* **8**, 600.

Flicek, P., Aken, B. L., Beal, K., Ballester, B., Caccamo, M., Chen, Y., Clarke, L., Coates, G., Cunningham, F., Cutts, T. et al. (2008). Ensembl 2008. *Nucleic Acids Res.* **36**, D707-D714.

Froldi, F., Ziosi, M., Tomba, G., Parisi, F., Garoia, F., Pession, A. and Grifoni, D. (2008). Drosophila lethal giant larvae neoplastic mutant as a genetic tool for cancer modeling. *Curr. Genomics* **9**, 147-154.

Froldi, F., Ziosi, M., Garoia, F., Pession, A., Grzeschik, N. A., Bellosta, P., Strand, D., Richardson, H. E. and Grifoni, D. (2010). The lethal giant larvae tumour suppressor mutation requires dMyc oncoprotein to promote clonal malignancy. *BMC Biol.* **8**, 33.

Gateff, E. (1978). Malignant neoplasms of genetic origin in Drosophila melanogaster. *Science* **200**, 1448-1459.

Griffiths-Jones, S., Grocock, R. J., van Dongen, S., Bateman, A. and Enright, A. J. (2006). miRBase: microRNA sequences, targets and gene nomenclature. *Nucleic Acids Res.* **34**, D140-D144.

Grifoni, D., Garoia, F., Schimanski, C. C., Schmitz, G., Laurenti, E., Galle, P. R., Pession, A., Cavicchi, S. and Strand, D. (2004). The human protein Hugl-1 substitutes for Drosophila lethal giant larvae tumour suppressor function in vivo. *Oncogene* **23**, 8688-8694.

Grifoni, D., Froldi, F. and Pession, A. (2013). Connecting epithelial polarity, proliferation and cancer in Drosophila: the many faces of lgl loss of function. *Int. J. Dev. Biol.* **57**, 677-687.

Grifoni, D., Sollazzo, M., Fontana, E., Froldi, F. and Pession, A. (2015). Multiple strategies of oxygen supply in Drosophila malignancies identify tracheogenesis as a novel cancer hallmark. *Sci. Rep.* **5**, 9061.

Grzeschik, N. A., Amin, N., Secombe, J., Brumby, A. M. and Richardson, H. E. (2007). Abnormalities in cell proliferation and apico-basal cell polarity are separable in Drosophila lgl mutant clones in the developing eye. *Dev. Biol.* **311**, 106-123.

Grzeschik, N. A., Parsons, L. M., Allott, M. L., Harvey, K. F. and Richardson, H. E. (2010a). Lgl, aPKC, and Crumbs regulate the Salvador/Warts/Hippo pathway through two distinct mechanisms. *Curr. Biol.* **20**, 573-581.

Grzeschik, N. A., Parsons, L. M. and Richardson, H. (2010b). Lgl, the SWH pathway and tumorigenesis: it's a matter of context & competition! *Cell Cycle* **9**, 3202-3212.

Hanahan, D. and Weinberg, R. A. (2011). Hallmarks of cancer: the next generation. *Cell* **144**, 646-674.

Henson, B. J., Bhattacharjee, S., O'Dee, D. M., Feingold, E. and Gollin, S. M. (2009). Decreased expression of miR-125b and miR-100 in oral cancer cells contributes to malignancy. *Genes Chromosomes Cancer* **48**, 569-582.

Hildebrandt, M. A. T., Gu, J., Lin, J., Ye, Y., Tan, W., Tamboli, P., Wood, C. G. and Wu, X. (2010). Hsa-miR-9 methylation status is associated with cancer development and metastatic recurrence in patients with clear cell renal cell carcinoma. *Oncogene* **29**, 5724-5728.

Huang, G.-S., Dai, L.-G., Yen, B. L. and Hsu, S.-H. (2011). Spheroid formation of mesenchymal stem cells on chitosan and chitosan-hyaluronan membranes. *Biomaterials* **32**, 6929-6945.

Huang, T., Sun, L., Yuan, X. and Qiu, H. (2017). Thrombospondin-1 is a multifaceted player in tumor progression. *Oncotarget* **8**, 84546-84558.

Humbert, P. O., Grzeschik, N. A., Brumby, A. M., Galea, R., Elsum, I. and Richardson, H. E. (2008). Control of tumourigenesis by the Scribble/Dlg/Lgl polarity module. *Oncogene* **27**, 6888-6907.

Hwang, H.-W. and Mendell, J. T. (2006). MicroRNAs in cell proliferation, cell death and tumorigenesis. *Br. J. Cancer* **94**, 776-780.

Imamura, N., Horikoshi, Y., Matsuzaki, T., Toriumi, K., Kitatani, K., Ogura, G., Masuda, R., Nakamura, N., Takekoshi, S. and Iwazaki, M. (2013). Localization of aPKC lambda/iota and its interacting protein, Lgl2, is significantly associated with lung adenocarcinoma progression. *Tokai J. Exp. Clin. Med.* **38**, 146-158.

Iorio, M. V. and Croce, C. M. (2012). microRNA involvement in human cancer. *Carcinogenesis* **33**, 1126-1133.

Ishizuka, A., Siomi, M. C. and Siomi, H. (2002). A *Drosophila* fragile X protein interacts with components of RNAi and ribosomal proteins. *Genes Dev.* **16**, 2497-2508.

Biology Open

Jin, P., Zarnescu, D. C., Ceman, S., Nakamoto, M., Mowrey, J., Jongens, T. A., Nelson, D. L., Moses, K. and Warren, S. T. (2004). Biochemical and genetic interaction between the fragile X mental retardation protein and the microRNA pathway. Nat. Neurosci. 7, 113-117.

John, B., Enright, A. J., Aravin, A., Tuschl, T., Sander, C. and Marks, D. S. (2004). Human MicroRNA targets. PLoS Biol. 2, e363.

Johnson, C. E., Gorringe, K. L., Thompson, E. R., Opeskin, K., Boyle, S. E., Wang, Y., Hill, P., Mann, G. B. and Campbell, I. G. (2012). Identification of copy number alterations associated with the progression of DCIS to invasive ductal carcinoma. Breast Cancer Res. Treat. 133, 889-898.

Kashyap, A., Zimmerman, T., Ergul, N., Bosserhoff, A., Hartman, U., Alla, V., Bataille, F., Galle, P. R., Strand, S. and Strand, D. (2012). The human Lgl polarity gene, Hugl-2, induces MET and suppresses Snail tumorigenesis. Oncogene 11, 1396-407.

Khan, S. J., Bajpai, A., Alam, M. A., Gupta, R. P., Harsh, S., Pandey, R. K., Goel-Bhattacharya, S., Nigam, A., Mishra, A. and Sinha, P. (2013). Epithelial neoplasia in Drosophila entails switch to primitive cell states. Proc. Natl. Acad. Sci. USA 110, E2163-E2172.

Kim, H., Choi, G. H., Na, D. C., Ahn, E. Y., Kim, G. I., Lee, J. E., Cho, J. Y., Yoo, J. E., Choi, J. S. and Park, Y. N. (2011). Human hepatocellular carcinomas with "Stemness"-related marker expression: keratin 19 expression and a poor prognosis. Hepatology 54, 1707-1717.

Klezovitch, O., Fernandez, T. E., Tapscott, S. J. and Vasioukhin, V. (2004). Loss of cell polarity causes severe brain dysplasia in Lgl1 knockout mice. Genes Dev. 18, 559-571.

Kucherenko, M. M., Barth, J., Fiala, A. and Shcherbata, H. R. (2012). Steroid-induced microRNA let-7 acts as a spatio-temporal code for neuronal cell fate in the developing Drosophila brain. EMBO J. 31, 4511-4523.

Kuphal, S., Wallner, S., Schimanski, C. C., Bataille, F., Hofer, P., Strand, S., Strand, D. and Bosserhoff, A. K. (2006). Expression of Hugl-1 is strongly reduced in malignant melanoma. Oncogene 25, 103-110.

Laffin, B., Wellberg, E., Kwak, H.-I., Burghardt, R. C., Metz, R. P., Gustafson, T., Schedin, P. and Porter, W. W. (2008). Loss of singleminded-2s in the mouse mammary gland induces an epithelial-mesenchymal transition associated with up-regulation of slug and matrix metalloprotease 2. Mol. Cell. Biol. 28, 1936-1946.

Laios, A., O'Toole, S., Flavin, R., Martin, C., Kelly, L., Ring, M., Finn, S. P., Barrett, C., Loda, M., Gleeson, N. et al. (2008). Potential role of miR-9 and miR-223 in recurrent ovarian cancer. Mol. Cancer 7, 35.

Lassmann, S., Weis, R., Makowiec, F., Roth, J., Danciu, M., Hopt, U. and Werner, M. (2007). Array CGH identifies distinct DNA copy number profiles of oncogenes and tumor suppressor genes in chromosomal- and microsatellite-unstable sporadic colorectal carcinomas. J. Mol. Med. 85, 293-304.

Lehmann, U., Hasemeier, B., Christgen, M., Müller, M., Römermann, D., Länger, F. and Kreipe, H. (2008). Epigenetic inactivation of microRNA gene hsa-mir-9-1 in human breast cancer. J. Pathol. 214, 17-24.

Li, B. H., Zhou, J. S., Ye, F., Cheng, X. D., Zhou, C. Y., Lu, W. G. and Xie, X. (2011). Reduced miR-100 expression in cervical cancer and precursors and its carcinogenic effect through targeting PLK1 protein. Eur. J. Cancer 47, 2166-2174.

Lisovsky, M., Dresser, K., Baker, S., Fisher, A., Woda, B., Banner, B. and Lauwers, G. Y. (2009). Cell polarity protein Lgl2 is lost or aberrantly localized in gastric dysplasia and adenocarcinoma: an immunohistochemical study. Mod. Pathol. 22, 977-984.

Lisovsky, M., Ogawa, F., Dresser, K., Woda, B. and Lauwers, G. Y. (2010). Loss of cell polarity protein Lgl2 in foveolar-type gastric dysplasia: correlation with expression of the apical marker aPKC-zeta. Virchows Arch. 457, 635-642.

Liu, Z., Sall, A. and Yang, D. (2008). MicroRNA: an emerging therapeutic target and intervention tool. Int. J. Mol. Sci. 9, 978-999.

Liu, X., Lu, D., Ma, P., Liu, H., Cao, Y., Sang, B., Zhu, X., Shi, Q., Hu, J., Yu, R. et al. (2015). Hugl-1 inhibits glioma cell growth in intracranial model. J. Neurooncol. 125, 113-121.

Lopez-Dee, Z. P., Chittur, S. V., Patel, H., Chinikaylo, A., Lippert, B., Patel, B., Lawler, J. and Gutierrez, L. S. (2015). Thrombospondin-1 in a murine model of colorectal carcinogenesis. PLoS ONE 10, e0139918.

Lujambio, A., Calin, G. A., Villanueva, A., Ropero, S., Sanchez-Cespedes, M., Blanco, D., Montuenga, L. M., Rossi, S., Nicoloso, M. S., Faller, W. J. et al. (2008). A microRNA DNA methylation signature for human cancer metastasis. Proc. Natl. Acad. Sci. USA 105, 13556-13561.

Luo, H., Zhang, H., Zhang, Z., Zhang, X., Ning, B., Guo, J., Nie, N., Liu, B. and Wu, X. (2009). Down-regulated miR-9 and miR-433 in human gastric carcinoma. J. Exp. Clin. Cancer Res. 28, 82.

Maere, S., Heymans, K. and Kuiper, M. (2005). BiNGO: a Cytoscape plugin to assess overrepresentation of gene ontology categories in biological networks. Bioinformatics 21, 3448-3449.

Matsuzaki, T., Takekoshi, S., Toriumi, K., Kitatani, K., Nitou, M., Imamura, N., Ogura, G., Masuda, R., Nakamura, N. and Iwazaki, M. (2015). Reduced expression of Hugl 1 contributes to the progression of lung squamous cell carcinoma. Tokai J. Exp. Clin. Med. 40, 169-177.

Merz, R., Schmidt, M., Török, I., Protin, U., Schuler, G., Walther, H. P., Krieg, F., Gross, M., Strand, D. and Mechler, B. M. (1990). Molecular action of the l(2)gl tumor suppressor gene of Drosophila melanogaster. Environ. Health Perspect. 88, 163-167.

Migliore, C., Martin, V., Leoni, V. P., Restivo, A., Atzori, L., Petrelli, A., Isella, C., Zorcolo, L., Sarotto, I., Casula, G. et al. (2012). MiR-1 downregulation cooperates with MACC1 in promoting MET overexpression in human colon cancer. Clin. Cancer Res. 18, 737-747.

Musch, A., Cohen, D., Yeaman, C., Nelson, W. J., Rodriguez-Boulan, E. and Brennwald, P. J. (2002). Mammalian homolog of Drosophila tumor suppressor lethal (2) giant larvae interacts with basolateral exocytic machinery in Madin-Darby canine kidney cells. Mol. Biol. Cell 13, 158-168.

Na, D. C., Lee, J. E., Yoo, J. E., Oh, B.-K., Choi, G. H. and Park, Y. N. (2011). Invasion and EMT-associated genes are up-regulated in B viral hepatocellular carcinoma with high expression of CD133-human and cell culture study. Exp. Mol. Pathol. 90, 66-73.

Nam, K. H., Kim, M. A., Choe, G., Kim, W. H. and Lee, H. S. (2014). Deregulation of the cell polarity protein Lethal giant larvae 2 (Lgl2) correlates with gastric cancer progression. Gastric Cancer 17, 610-620.

O'Hara, A. J., Wang, L., Dezube, B. J., Harrington, W. J., Jr, Damania, B. and Dittmer, D. P. (2009). Tumor suppressor microRNAs are underrepresented in primary effusion lymphoma and Kaposi sarcoma. Blood 113, 5938-5941.

Ohshiro, T., Yagami, T., Zhang, C. and Matsuzaki, F. (2000). Role of cortical tumour-suppressor proteins in asymmetric division of Drosophila neuroblast. Nature 408, 593-596.

Pan, Y.-Z., Morris, M. E. and Yu, A.-M. (2009). MicroRNA-328 negatively regulates the expression of breast cancer resistance protein (BCRP/ABCG2) in human cancer cells. Mol. Pharmacol. 75, 1374-1379.

Parrish, R. S. and Spencer, H. J.III. (2004). Effect of normalization on significance testing for oligonucleotide microarrays. J. Biopharm. Stat. 14, 575-589.

Parsons, L. M., Portela, M., Grzeschik, N. A. and Richardson, H. E. (2014). Lgl regulates Notch signaling via endocytosis, independently of the apical aPKC-Par6-Baz polarity complex. Curr. Biol. 24, 2073-2084.

Parsons, L. M., Grzeschik, N. A., Amaratunga, K., Burke, P., Quinn, L. M. and Richardson, H. E. (2017). A Kinome RNAi Screen in Drosophila Identifies Novel Genes Interacting with Lgl, aPKC, and Crb Cell Polarity Genes in Epithelial Tissues. G3 (Bethesda) 7, 2497-2509.

Pasquinelli, A. E., Reinhart, B. J., Slack, F., Martindale, M. Q., Kuroda, M. I., Maller, B., Hayward, D. C., Ball, E. E., Degnan, B., Müller, P. et al. (2000). Conservation of the sequence and temporal expression of let-7 heterochronic regulatory RNA. Nature 408, 86-89.

Peng, C.-Y., Manning, L., Albertson, R. and Doe, C. Q. (2000). The tumour-suppressor genes lgl and dlg regulate basal protein targeting in Drosophila neuroblasts. Nature 408, 596-600.

Portela, M., Parsons, L. M., Grzeschik, N. A. and Richardson, H. E. (2015). Regulation of Notch signaling and endocytosis by the Lgl neoplastic tumor suppressor. Cell Cycle 14, 1496-1506.

Reiner, A., Yekutieli, D. and Benjamini, Y. (2003). Identifying differentially expressed genes using false discovery rate controlling procedures. Bioinformatics 19, 368-375.

Rodriguez-Manzaneque, J. C., Lane, T. F., Ortega, M. A., Hynes, R. O., Lawler, J. and Iruela-Arispe, M. L. (2001). Thrombospondin-1 suppresses spontaneous tumor growth and inhibits activation of matrix metalloproteinase-9 and mobilization of vascular endothelial growth factor. Proc. Natl. Acad. Sci. USA 98, 12485-12490.

Rothé, F., Ignatiadis, M., Chaboteaux, C., Haibe-Kains, B., Kheddoumi, N., Majjaj, S., Badran, B., Fayyad-Kazan, H., Desmedt, C., Harris, A. L. et al. (2011). Global microRNA expression profiling identifies MiR-210 associated with tumor proliferation, invasion and poor clinical outcome in breast cancer. PLoS ONE 6, e20980.

Russ, A., Louderbough, J. M. V., Zarnescu, D. and Schroeder, J. A. (2012). Hugl1 and hugl2 in mammary epithelial cells: polarity, proliferation, and differentiation. PLoS ONE 7, e47734.

Sablina, A. A., Chen, W., Arroyo, J. D., Corral, L., Hector, M., Bulmer, S. E., DeCaprio, J. A. and Hahn, W. C. (2007). The tumor suppressor PP2A Abeta regulates the RalA GTPase. Cell 129, 969-982.

Safran, M., Dalah, I., Alexander, J., Rosen, N., Iny Stein, T., Shmoish, M., Nativ, N., Bahir, I., Doniger, T., Krug, H. et al. (2010). GeneCards Version 3: the human gene integrator. Database 2010, baq020.

Sampson, V. B., Rong, N. H., Han, J., Yang, Q., Aris, V., Soteropoulos, P., Petrelli, N. J., Dunn, S. P. and Krueger, L. J. (2007). MicroRNA let-7a down-regulates MYC and reverts MYC-induced growth in Burkitt lymphoma cells. Cancer Res. 67, 9762-9770.

Scheel, C. and Weinberg, R. A. (2012). Cancer stem cells and epithelial-mesenchymal transition: concepts and molecular links. Semin. Cancer Biol. 22, 396-403.

Schimanski, C. C., Schmitz, G., Kashyap, A., Bosserhoff, A. K., Bataille, F., Schäfer, S. C., Lehr, H. A., Berger, M. R., Galle, P. R., Strand, S. et al. (2005). Reduced expression of Hugl-1, the human homologue of Drosophila tumour suppressor gene lgl, contributes to progression of colorectal cancer. Oncogene 24, 3100-3109.

Selbach, M., Schwanhäusser, B., Thierfelder, N., Fang, Z., Khanin, R. and Rajewsky, N. (2008). Widespread changes in protein synthesis induced by microRNAs. Nature 455, 58-63.

Selcuklu, S. D., Donoghue, M. T. A., Rehmet, K., de Souza Gomes, M., Fort, A., Kovvuru, P., Muniyappa, M. K., Kerin, M. J., Enright, A. J. and Spillane, C. (2012). MicroRNA-9 inhibition of cell proliferation and identification of novel miR-9 targets by transcriptome profiling in breast cancer cells. J. Biol. Chem. 287, 29516-29528.

Sempere, L. F., Christensen, M., Silahtaroglu, A., Bak, M., Heath, C. V., Schwartz, G., Wells, W., Kauppinen, S. and Cole, C. N. (2007). Altered MicroRNA expression confined to specific epithelial cell subpopulations in breast cancer. Cancer Res. 67, 11612-11620.

Shannon, P., Markiel, A., Ozier, O., Baliga, N. S., Wang, J. T., Ramage, D., Amin, N., Schwikowski, B. and Ideker, T. (2003). Cytoscape: a software environment for integrated models of biomolecular interaction networks. Genome Res. 13, 2498-2504.

Shi, W., Alajez, N. M., Bastianutto, C., Hui, A. B., Mocanu, J. D., Ito, E., Busson, P., Lo, K. W., Ng, R., Waldron, J. et al. (2010). Significance of Plk1 regulation by miR-100 in human nasopharyngeal cancer. Int. J. Cancer 126, 2036-2048.

Song, J., Peng, X. L., Ji, M. Y., Ai, M. H., Zhang, J. X. and Dong, W. G. (2013). Hugl-1 induces apoptosis in esophageal carcinoma cells both in vitro and in vivo. World J. Gastroenterol. 19, 4127-4136.

Spaderna, S., Schmalhofer, O., Wahlbuhl, M., Dimmler, A., Bauer, K., Sultan, A., Hlubek, F., Jung, A., Strand, D., Eger, A. et al. (2008). The transcriptional repressor ZEB1 promotes metastasis and loss of cell polarity in cancer. Cancer Res. 68, 537-544.

Spieker, N., van Sluis, P., Beitsma, M., Boon, K., van Schaik, B. D. C., van Kampen, A. H. C., Caron, H. and Versteeg, R. (2001). The MEIS1 oncogene is highly expressed in neuroblastoma and amplified in cell line IMR32. Genomics 71, 214-221.

Sripathy, S., Lee, M. and Vasioukhin, V. (2011). Mammalian Llgl2 is necessary for proper branching morphogenesis during placental development. Mol. Cell. Biol. 31, 2920-2933.

Strand, D., Jakobs, R., Merdes, G., Neumann, B., Kalmes, A., Heid, H. W., Husmann, I. and Mechler, B. M. (1994). The Drosophila lethal(2)giant larvae tumor suppressor protein forms homo-oligomers and is associated with nonmuscle myosin II heavy chain. J. Cell Biol. 127, 1361-1373.

Strand, D., Unger, S., Corvi, R., Hartenstein, K., Schenkel, H., Kalmes, A., Merdes, G., Neumann, B., Krieg-Schneider, F., Coy, J. F. et al. (1995). A human homologue of the Drosophila tumour suppressor gene l(2)gl maps to 17p11.2-12 and codes for a cytoskeletal protein that associates with nonmuscle myosin II heavy chain. Oncogene 11, 291-301.

Streit, M., Riccardi, L., Velasco, P., Brown, L. F., Hawighorst, T., Bornstein, P. and Detmar, M. (1999). Thrombospondin-2: a potent endogenous inhibitor of tumor growth and angiogenesis. Proc. Natl. Acad. Sci. USA 96, 14888-14893.

Suh, Y. S., Bhat, S., Hong, S.-H., Shin, M., Bahk, S., Cho, K. S., Kim, S.-W., Lee, K.-S., Kim, Y.-J., Jones, W. D. et al. (2015). Genome-wide microRNA screening reveals that the evolutionary conserved miR-9a regulates body growth by targeting sNPFR1/NPYR. Nat. Commun. 6, 7693.

Takamizawa, J., Konishi, H., Yanagisawa, K., Tomida, S., Osada, H., Endoh, H., Harano, T., Yatabe, Y., Nagino, M., Nimura, Y. et al. (2004). Reduced expression of the let-7 microRNAs in human lung cancers in association with shortened postoperative survival. Cancer Res. 64, 3753-3756.

Tanentzapf, G. and Tepass, U. (2003). Interactions between the crumbs, lethal giant larvae and bazooka pathways in epithelial polarization. Nat. Cell Biol. 5, 46-52.

Tavazoie, S. F., Alarcón, C., Oskarsson, T., Padua, D., Wang, Q., Bos, P. D., Gerald, W. L. and Massagué, J. (2008). Endogenous human microRNAs that suppress breast cancer metastasis. Nature 451, 147-152.

To, K. K. W., Zhan, Z., Litman, T. and Bates, S. E. (2008). Regulation of ABCG2 expression at the 3′ untranslated region of its mRNA through modulation of transcript stability and protein translation by a putative microRNA in the S1 colon cancer cell line. Mol. Cell. Biol. 28, 5147-5161.

To, K. K. W., Robey, R. W., Knutsen, T., Zhan, Z., Ried, T. and Bates, S. E. (2009). Escape from hsa-miR-519c enables drug-resistant cells to maintain high expression of ABCG2. Mol. Cancer Ther. 8, 2959-2968.

Tränkenschuh, W., Puls, F., Christgen, M., Albat, C., Heim, A., Poczkaj, J., Fleming, P., Kreipe, H. and Lehmann, U. (2010). Frequent and distinct aberrations of DNA methylation patterns in fibrolamellar carcinoma of the liver. PLoS ONE 5, e13688.

Tsuchiya, S., Fujiwara, T., Sato, F., Shimada, Y., Tanaka, E., Sakai, Y., Shimizu, K. and Tsujimoto, G. (2011). MicroRNA-210 regulates cancer cell proliferation through targeting fibroblast growth factor receptor-like 1 (FGFRL1). J. Biol. Chem. 286, 420-428.

Tsuruga, T., Nakagawa, S., Watanabe, M., Takizawa, S., Matsumoto, Y., Nagasaka, K., Sone, K., Hiraike, H., Miyamoto, Y., Hiraike, O. et al. (2007). Loss of Hugl-1 expression associates with lymph node metastasis in endometrial cancer. Oncol. Res. 16, 431-435.

Ventura, A. and Jacks, T. (2009). MicroRNAs and cancer: short RNAs go a long way. Cell 136, 586-591.

Volinia, S., Calin, G. A., Liu, C.-G., Ambs, S., Cimmino, A., Petrocca, F., Visone, R., Iorio, M., Roldo, C., Ferracin, M. et al. (2006). A microRNA expression signature of human solid tumors defines cancer gene targets. Proc. Natl. Acad. Sci. USA 103, 2257-2261.

Walker, J. A., Tchoudakova, A. V., McKenney, P. T., Brill, S., Wu, D., Cowley, G. S., Hariharan, I. K. and Bernards, A. (2006). Reduced growth of Drosophila neurofibromatosis 1 mutants reflects a non-cell-autonomous requirement for GTPase-Activating Protein activity in larval neurons. Genes Dev. 20, 3311-3323.

Wettenhall, J. M. and Smyth, G. K. (2004). limmaGUI: a graphical user interface for linear modeling of microarray data. Bioinformatics 20, 3705-3706.

Wong, P., Iwasaki, M., Somervaille, T. C. P., So, C. W. E. and Cleary, M. L. (2007). Meis1 is an essential and rate-limiting regulator of MLL leukemia stem cell potential. Genes Dev. 21, 2762-2774.

Woodhouse, E., Hersperger, E., Stetler-Stevenson, W. G., Liotta, L. A. and Shearn, A. (1994). Increased type IV collagenase in lgl-induced invasive tumors of Drosophila. Cell Growth Differ. 5, 151-159.

Woodhouse, E., Hersperger, E. and Shearn, A. (1998). Growth, metastasis, and invasiveness of Drosophila tumors caused by mutations in specific tumor suppressor genes. Dev. Genes Evol. 207, 542-550.

Wu, Y.-C., Chen, C.-H., Mercer, A. and Sokol, N. S. (2012). Let-7-complex microRNAs regulate the temporal identity of Drosophila mushroom body neurons via chinmo. Dev. Cell 23, 202-209.

Yao, I., Takagi, H., Ageta, H., Kahyo, T., Sato, S., Hatanaka, K., Fukuda, Y., Chiba, T., Morone, N., Yuasa, S. et al. (2007). SCRAPPER-dependent ubiquitination of active zone protein RIM1 regulates synaptic vesicle release. Cell 130, 943-957.

Yu, F., Yao, H., Zhu, P., Zhang, X., Pan, Q., Gong, C., Huang, Y., Hu, X., Su, F., Lieberman, J. et al. (2007). let-7 regulates self renewal and tumorigenicity of breast cancer cells. Cell 131, 1109-1123.

Yuan, Z.-R., Wang, R., Solomon, J., Luo, X., Sun, H., Zhang, L. and Shi, Y. (2005). Identification and characterization of survival-related gene, a novel cell survival gene controlling apoptosis and tumorigenesis. Cancer Res. 65, 10716-10724.

Zarnescu, D. C., Jin, P., Betschinger, J., Nakamoto, M., Wang, Y., Dockendorff, T. C., Feng, Y., Jongens, T. A., Sisson, J. C., Knoblich, J. A. et al. (2005). Fragile X protein functions with lgl and the par complex in flies and mice. Dev. Cell 8, 43-52.

Zhang, H., Qi, M., Li, S., Qi, T., Mei, H., Huang, K., Zheng, L. and Tong, Q. (2012). microRNA-9 targets matrix metalloproteinase 14 to inhibit invasion, metastasis, and angiogenesis of neuroblastoma cells. Mol. Cancer Ther. 11, 1454-1466.

Zhou, S., Schuetz, J. D., Bunting, K. D., Colapietro, A.-M., Sampath, J., Morris, J. J., Lagutina, I., Grosveld, G. C., Osawa, M., Nakauchi, H. et al. (2001). The ABC transporter Bcrp1/ABCG2 is expressed in a wide variety of stem cells and is a molecular determinant of the side-population phenotype. Nat. Med. 7, 1028-1034.

Zinovieva, R. D., Duncan, M. K., Johnson, T. R., Torres, R., Polymeropoulos, M. H. and Tomarev, S. I. (1996). Structure and chromosomal localization of the human homeobox gene Prox 1. Genomics 35, 517-522.